REPUBLIC OF TÜRKİYE

ALTINBAŞ UNIVERSITY

Institute of Graduate Studies

Mechanical Engineering

INVESTIGATION OF EFFECTIVE FACTORS OF A SOLAR POWERED FIXED-WING UAV FOR ENHANCED ENDURANCE AND EFFICIENCY

Wajeeha RAJAB

Master's Thesis

Supervisor

Asst. Prof. Dr. Yaser ALAIWI

İstanbul, 2024

INVESTIGATION OF EFFECTIVE FACTORS OF A SOLAR POWERED FIXED-WING UAV FOR ENHANCED ENDURANCE AND EFFICIENCY

Wajeeha RAJAB

Mechanical Engineering

Master's Thesis

ALTINBAŞ UNIVERSITY

2024

The thesis titled INVESTIGATION OF EFFECTIVE FACTORS OF A SOLAR POWERED FIXED-WING UAV FOR ENHANCED ENDURANCE AND EFFICIENCY prepared by WAJEEHA RAJAB and submitted on 09/01/2024 has been **accepted unanimously** for the degree of Master of Science in Mechanical Engineering

Asst. Prof. Dr. Yaser ALAIWI
Supervisor

Thesis Defense Committee Members:

Asst. Prof. Dr. Yaser ALAIWI	Department of Mechanical Engineering, Altınbaş University	
Asst. Prof. Dr. İbrahim KOÇ	Department of Mechanical Engineering, Altınbaş University	
Asst. Prof. Dr. Haydar İzzettin KEPEKÇİ	Department of Mechatronics Engineering, Istanbul Gelişim University	

I hereby declare that this thesis meets all format and submission requirements for a master's thesis.

I hereby declare that all information/data presented in this graduation project has been obtained in full accordance with academic rules and ethical conduct. I also declare all unoriginal materials and conclusions have been cited in the text and all references mentioned in the Reference List have been cited in the text, and vice versa as required by the abovementioned rules and conduct.

Wajeeha RAJAB

Signature

ABSTRACT

INVESTIGATION OF EFFECTIVE FACTORS OF A SOLAR POWERED FIXED-WING UAV FOR ENHANCED ENDURANCE AND EFFICIENCY

RAJAB, Wajeeha

M.Sc., Mechanical Engineering, Altınbaş University,

Supervisor: Asst. Prof. Dr. Yaser ALAIWI

Date: 01 / 2024

Pages: 63

This research aims to investigate effective factors for enhancing the performance and efficiency of fixed-wing solar-powered unmanned aerial vehicles (UAVs). The MQ-9 model was selected for analysis. SunPower C60 solar cells were integrated onto the entire wing surface through computer-aided design using SolidWorks. Calculations quantified additional energy harnessed, battery capacity for storage, and improvements in flight endurance and range. Findings reveal that augmenting the MQ-9 wings with high-efficiency photovoltaic cells substantially increased the solar-powered UAV's flight duration by approximately 30%. Conclusions confirm incorporating renewable solar energy enables notable efficiency gains in fixed-wing UAVs. This study paves the path for solar technology integration, moving towards environmentally sustainable aviation systems. Further work should assess cutting-edge solar cells, improved energy storage, extended operational flight times, and broader aerospace applications. In summary, by highlighting the immense potential of solar power in enhancing fixed-wing UAV efficiency. This research advocates solar-powered systems as pioneers for the future of unmanned flight technology.

Keywords: UAV, Solar Cells, High Efficiency, Solar Power, Fixed Wing, Analysis.

TABLE OF CONTENTS

LIST OF TABLES

Pages

LIST OF FIGURES

Pages

ABBREVIATIONS

UAV	:	Unmanned Aerial Vehicle
SPUAV	:	Solar Powered Unmanned Aerial Vehicle
CFD	:	Computational Fluid Dynamics
MPPT	:	Maximum Power Point Tracking
PV	:	Photovoltaic
HALE	:	High Altitude Long Endurance
VTOL	:	Vertical Take-Off and Landing
IUAV	:	Integrated UAV
IPBDO	:	Possibility-Based Design Optimisation
EMS	:	Energy Management Strategy
HPS	:	Hybrid-Powered Systems
MDAO	:	Multi-Disciplinary Analysis and Optimization
LDA	:	Latent Dirichlet Allocation
SBE	:	Simple Blade Element
WSN	:	Wireless Sensor Network

LIST OF SYMBOLS

V	:	Fluid Velocity
p	:	Fluid Pressure
V_V	:	Constant Related To The Condensing Side
ρ	:	Fluid Density
C_L	:	Lift Coefficient
C_D	:	Drag Coefficient
S	:	Surface Area
T	:	Thrust Force
D	:	Drag Force
L	:	Lift Force
θ	:	Angle
C_R	:	Gravity Coefficient
η_{Solar}	:	Solar Cell Efficiency
η_{Manager}	:	Efficiency Of DC/DC Converter
P_{Need}	:	Total Power Consumption
P_{Solar}	:	Solar Power
Q_{Battery}	:	Battery Energy Storage
E_{Day}	:	Solar Energy Collected Per Day
k_{Solar}	:	Solar Cell Surface Density
S_{Solar}	:	Solar Cell Surface Area
k_{Battary}	:	Battery Weight-Energy Ratio
k_{prop}	:	Propulsion System Weight Constant
$P_{Payload}$	:	Payload Power

1. INTRODUCTION

1.1 BRIEF BACKGROUND

The development of Unmanned Aerial Vehicles (UAVs), commonly called drones, highlights major advancements in air technology. The journey of UAV technology began in the 19th century, notably with Alfred Nobel's innovative experiment in 1896 when he mounted a camera on a rocket. This marked the start of using unmanned methods for aerial observation [1]. Significant progress in the UAV domain became more pronounced in the early 20th century, particularly during World War I. A key breakthrough occurred in 1917 when American inventor Elmer Sperry introduced the first autopilot control system. This was a critical step in the development of aircraft for military purposes, marking the beginning of UAV use in combat and reconnaissance, which would set the stage for their future roles in military operations [2], [3] . The years between World War I and World War II, as well as during the latter, witnessed continuous advancements in UAV technology. British-born actor Reginald Denny, who had served in the Royal Flying Corps during the first World War, developed a strong interest in radio-controlled aircraft in the 1930s. His contributions greatly accelerated the progress in the UAV field, leading to the emergence of new companies and research dedicated to the development of UAVs [3]. An important milestone in the history of UAVs was their extensive use during the Vietnam War. This period saw the most widespread application of UAVs to that point, as technological enhancements made these vehicles more adaptable and effective for diverse military operations [4].The Vietnam War demonstrated the growing relevance of UAVs in modern warfare and their potential for various uses. In recent times, the advancement in UAV technology has been fueled by factors such as lower costs of development, improved flight capabilities, and technological innovations including GPS, cameras, and sensors. These advancements have extended the use of UAVs beyond military purposes to civil and non-military fields like package delivery, aerial surveying, farming, and wildlife preservation [5]. The growth of UAVs represents not only a story of technological development but also reflects the changing approaches in military strategy and the increasing use of automation across various industries. The evolution of UAVs from basic early models to complex, sophisticated systems demonstrate the dynamic nature of technological advancements and their impact in both military and civilian spheres.

1.2 MOTIVATION

i. Addressing Global Energy Challenges:

The urgency of shifting towards sustainable energy solutions in aviation technology, especially in UAVs, forms the core motivation for this research. This study addresses the global need for renewable energy sources, focusing on the integration of solar technology in UAVs as a response to the increasing scarcity and environmental impact of fossil fuels.

ii. Enhancing UAV Endurance and Efficiency:

The research is driven by the goal of significantly improving the endurance and operational efficiency of UAVs. By integrating SunPower C60 photovoltaic cells onto the wings of the MQ-9 UAV, this study aims to extend the UAV's flight duration by approximately 30%. This enhancement is crucial for applications requiring long-duration flights and continuous operations.

iii. Pioneering in Technological Innovation:

A key motivation is to contribute to the advancement of UAV technology through innovative applications. Incorporating solar energy into UAVs represents a groundbreaking step in UAV design, setting a precedent for future developments in the field and potentially revolutionizing how UAVs are powered.

iv. Promoting Environmental Sustainability:

This research is inspired by the need to promote environmental sustainability in aviation. By harnessing solar energy, the study aims to reduce the carbon footprint of UAV operations, aligning with global efforts towards ecological preservation and sustainable development.

1.3 THESIS OBJECTIVES

i. To design and develop an innovative solar-powered fixed-wing UAV model integrated with SunPower C60 photovoltaic cells to significantly enhance flight endurance and efficiency.

ii. To conduct in-depth analysis of the impact of solar panel integration on the UAV’s operational duration, range capabilities, and overall performance.

iii. To promote the adoption of solar technology as a sustainable power source for UAV systems, supporting global aviation environmental preservation efforts.

iv. To establish solar-powered UAVs as pioneers in renewable energy applications for unmanned vehicles, serving as benchmarks for further advancements in the technological domain.

1.4 THESIS STRUCTURE

In Chapter 1, a comprehensive background on the evolution of unmanned aerial vehicles (UAVs) is provided. This chapter also presents the key motivations behind this research study and states the main objectives of developing an innovative solar-powered fixed-wing UAV model targeting enhanced efficiency.

In Chapter 2, an in-depth analysis and discussion of previous scholarly works related to solar-powered UAVs is conducted. This literature review encompasses topics such as optimizing UAV designs, applications in air quality monitoring, delivery systems, energy management strategies, and addressing the challenges of continuous flight.

In Chapter 3, a detailed outline of the research methodology is presented. This covers foundational information regarding aerodynamics and solar power calculations relevant to modeling the selected UAV prototype. The steps for integrating solar panels onto the wings of the MQ-9 UAV are also delineated.

In Chapter 4, the results obtained after incorporating solar cells onto the wings of the MQ-9 model are thoroughly examined. Calculations regarding the additional solar energy harnessed are provided. The improvements in the UAV's endurance and efficiency are quantified and discussed.

In Chapter 5, the key conclusions derived from the extensive research study are summarized. Additionally, recommendations for potential future work to further advance solar-powered UAV technology are suggested.

2. LITERATURE REVIEW

Unmanned aerial vehicles (UAVs) represent a rapidly evolving sector within the global aerospace industry, poised for substantial growth throughout this decade. These versatile technological platforms are gaining prominence across various facets of modern society. As UAVs play a pivotal role in fostering growth and enhancing competitiveness within the aerospace industry, substantial investments, amounting to billions of dollars, have been dedicated to their development in advanced economies. Despite the swift proliferation of UAVs, there exists a scarcity of comprehensive studies that categorize UAV technologies into distinct components or delve into the trajectories of their technological advancements [6].

This study employs the latent Dirichlet allocation (LDA) technique, incorporating topic modeling and network analysis, to investigate the prevailing technological trends and the broader technological portfolio associated with UAVs. The dataset comprises UAV patents sourced from the Korea Intellectual Property Rights Information Service. Analysis of the findings reveals that communication technology occupies a predominant share at 34.1%, followed by power supply at 19.5%, and navigation systems at 17.6% among the identified technological topics. The technological portfolio of UAVs can be categorized into three main groups: control systems, operational systems, and devices [7].

This research serves as a valuable reference for UAV developers and policymakers, offering insights into the prevailing technological landscape of UAVs and aiding in informed decision-making for the continued growth and integration of UAV technologies into various domains [8].

In a past article, the enhanced design of a solar-powered UAV, dubbed SUAV:Q, was explored. Aerial robot applications frequently face a dilemma when choosing an airframe. Fixed-wing small-scale UAVs struggle with low-altitude surveys, whereas quadrotor UAVs, despite their agility, have restricted flight durations. An earlier design introduced a solar-powered aerial vehicle that could shift between fixed-wing and quad-rotor modes, harnessing excess energy from the fixed-wing mode for its quad-rotor operations. This paper unveils refinements in the robot's design, highlighting a modular structure, a refined hybrid propulsion mechanism, and sophisticated solar electronics. Two models were developed for evaluation in both configurations. The efficacy of the solar electronics and propulsion systems was validated using both simulations and real-world data from the prototypes [9] .

In one of previous studies, the potential of Small Unmanned Aerial Vehicles (SUAVs) for urban air quality monitoring was explored. It was found that SUAVs can be effectively used for this purpose, offering a cost-effective and flexible solution. The study highlighted the importance of considering the aerodynamic effects on the sensors, as they can impact the accuracy of the measurements. The use of Computational Fluid Dynamics (CFD) was suggested to better understand these effects [10].

In past reaserch, the market of solar-powered Unmanned Aerial Vehicles (UAVs) for defense purposes and drone services was projected to grow significantly in the next decade. The main challenge identified was the scalability of the proposed architectures to increase payload capabilities. The paper introduced the concept of using box-wing and tandem-wing architectures for these UAVs. It was shown that the presence of wing tip joiners can offer aeroelastic benefits. The study utilized an in-house developed Multi-Disciplinary Analysis and Optimization (MDAO) code and the open-source aeroelastic code ASWING. The results indicated that while the aerodynamic advantages of the box-wing were marginal, significant advantages were observed from the aeroelastic analyses. If the joiners were removed from the box-wing configuration, it was found that the safety margin from flutter speed was reduced by half [11].

In a prervious discussed paper, the systematic development of a solar electric powered UAV (Unmanned Aerial Vehicle) was presented. Emphasis was placed on proving the feasibility of key engineering techniques for future large-scale high-altitude solar-powered UAVs. A design resembling a sailplane was adopted, characterized by a high aspect ratio wing, slender fuselage, and a tail boom. Through the application of lifting line theory, the aerodynamic geometry and performance were designed and subsequently verified using the AVL code. A combination of materials, including composite and balsa, was chosen to ensure the structure's lightweight nature and rigidity. The incorporation of fragile photovoltaic cells onto the wing's surface was described, and their collaboration with a lithium-polymer secondary battery was highlighted. The development and implementation of an onboard power management device were also detailed. Ground and flight tests were conducted, during which the aerodynamic performance, the power supply capability of the solar array, and the efficiency of the power management device were validated. The findings revealed an efficiency exceeding 85% for the power management device, a power requirement under 80 W for straight and level flight, and the need for a minimum solar radiation of 650 W/m2 for solar-only level flight. The achievement of all design objectives was confirmed [12].

In this research, solar-powered airplanes were studied. The consumption of solar energy by these airplanes, as an alternative to traditional fossil fuels, was highlighted. A review of the historical development of solar-powered airplanes was provided. Notable prototypes, especially those sponsored by the government, were detailed. The potential future applications of these airplanes in both civilian and military fields were proposed. The study concluded by discussing the challenges faced by solar-powered airplanes, emphasizing that while they hold promise as alternatives to some current technologies, they still require further development and face significant technical obstacles [13].

In a previous article the development of an optimal path planning strategy for solar-powered UAVs using unit quaternions was discussed. The significance of efficient path planning for maximizing solar energy absorption and extending UAV endurance was highlighted. Through the proposed quaternion-based approach, the UAV's orientation was optimized to ensure maximum exposure to sunlight. Results indicated a notable enhancement in the UAV's operational duration and energy efficiency when following the optimized path [14].

In the research titled "The Effect of Use of Solar Panels on Micro Scale Fixed-Wing UAV Type as A Power Recharging System", the impact of integrating solar panels into micro-scale fixed-wing UAVs was explored. It was identified that drones of this type often have limited flight time due to battery constraints. To address this limitation, solar panels were added to the wings of the UAV. The solar cells utilized were SunPower C60, arranged in a series of 10 with a maximum efficiency of 21%. The results demonstrated that the micro-scale UAV, when equipped with solar panels, could extend its flight time by 2 minutes under an average solar radiation intensity of 929.46 W/m2. During the flight tests, the solar cells were observed to produce an average power of 15.14 W with a peak efficiency of 14.8%, leading to a total flight time of 15 minutes. This research confirmed the feasibility of augmenting micro-scale fixed-wing UAVs with solar panels [15].

In a past study, the conceptual design, development, and flight testing of AtlantikSolar, a solar-powered Low-Altitude Long-Endurance (LALE) Unmanned Aerial Vehicle (UAV) built at ETH Zurich, was presented in this paper. This UAV was designed to provide perpetual endurance at a specific geographic latitude during a 4-month window centered around June 21st. An improved design method was introduced to enhance flight robustness against local meteorological disturbances. The UAV's capabilities were demonstrated through a 12-hour flight that relied solely on batteries, simulating night-flight conditions. Additionally, results from Search-And-Rescue field trials were presented, where a camera and processing pod were used to create high-fidelity 3D-maps of a simulated disaster area [16].

In past research presented, the potential of unmanned aerial vehicles (UAVs) for urban goods delivery was explored. Challenges posed by the limited endurance of UAVs due to onboard energy constraints were highlighted. The high costs associated with building UAV charging stations were identified as a barrier to dense deployment. Solar-powered UAVs were introduced as a solution, eliminating the need for charging stations by harnessing solar power during the day. A system was proposed wherein solar-powered UAVs, when low on power, would recharge at landing places provided by customers. Advanced path planning algorithms were introduced to minimize mission time in environments with static charging efficiency. The study also delved into routing in dynamic charging efficiency environments, proposing mission arrangement protocols. Simulation results indicated that the proposed algorithms outperformed existing UAV path planning algorithms in solar-powered UAV systems [17].

The development and integration of a solar-powered UAV with a Wireless Sensor Network (WSN) for remote gas sensing were explored in the discussed article. Emphasis was placed on the potential of such UAVs for long-duration missions. The UAV's capability to operate in remote areas and provide real-time data was highlighted. Successful flight tests were conducted, demonstrating the UAV's efficiency and the integrated system's potential for remote gas sensing applications [18].

In recent years, the development of solar-powered high-altitude UAVs has been given increased attention. The article proposed a novel approach to eliminate the need for landing gear by landing the UAV on a mobile ground vehicle. This method was suggested to not only enhance payload capacity but also to simplify landings under crosswind conditions, thereby increasing operational availability. A system comprising a small UAV and a car-mounted landing platform was prepared as a technology demonstrator. Both simulations and real experiments were conducted, with the results showcasing the feasibility of such landings [19].

In a previous paper, the unique capabilities of unmanned solar-powered aircraft were discussed, noting their achievements in setting general aviation records for continuous flight duration and sustained altitude. The exploration of solar-powered flight for small-scale unmanned aerial vehicles (UAVs) was identified as a relatively uncharted area of research. By harnessing solar energy, these small-scale UAVs were found capable of supporting more robust sensor payloads and extending flight durations beyond 24 hours, potentially achieving multi-day flights. The paper emphasized the recent advancements made by the Center for Distributed Robotics on a solar UAV with a four-meter wingspan, tailored for low-altitude aerial sensing tasks. Key design elements related to the airframe, propulsion, and electronics were presented, along with experiments that assessed the performance of the solar power system and the airframe [20].

In previous research, an increasing fascination with aerial robotic platforms for tasks like sensing, monitoring, and transportation was underscored. The significance of unmanned aerial vehicles (UAVs) in these domains was emphasized, with the inherent challenges of both fixed-wing and multi-rotor UAVs being pointed out. Fixed-wing UAVs were depicted as apt for high-altitude monitoring and prolonged flights, whereas the dexterity and close-proximity surveying capabilities of quadrotors were highlighted. Drawing from earlier work, a trio of refined prototypes was introduced in the study. The distinct attributes of solar-powered fixed-wing flight, quad-rotor dynamics, and the transformative features of the SUAV: Q platform were explored through these designs. Upgrades in the transformation process, the design of the airframe, the variable pitch propulsion mechanism, and tailored power electronics were elaborated upon. Through empirical evaluations, the effectiveness of these design alterations was validated [21].

In previous research, the challenges faced by high-altitude, long-endurance solar-powered UAVs, particularly those with high-aspect-ratio wings, were discussed. It was observed that the wingtips of these UAVs were highly susceptible to deformation, and their flutter velocities were notably low, making them vulnerable to gust loads. Despite the critical nature of ensuring the structural safety of these UAVs in flight, no established design criteria existed for the structural design of solar-powered UAVs. Addressing this gap, the study introduced design criteria for structural safety, tailored to the unique characteristics of large aspect ratio solar-powered UAVs. The structural integrity of these UAVs was examined in terms of static strength, stiffness, and dynamic load. Computational findings indicated that, during cruising, the peak stress experienced by the UAV's structure was significantly below the material's breaking strength. However, persistent vibrations from flutter could induce substantial overloads, potentially resulting in fatigue and structural damage. Under gust conditions, the structural response was found to stabilize quickly. Yet, beyond a specific flight speed, any gust could trigger a rapid structural divergence, leading to swift structural failure. The research also highlighted that the combined effects of bending, twisting, and lateral oscillations in the high-aspect-ratio wings could culminate in structural flutter damage [22].

In previous research, the varied characteristics of solar drones operating in different spatial conditions were examined. It was observed that drones flying at low altitudes were commonly chosen for mapping tasks, attributed to their adaptability and ease of movement. In contrast, drones that operated at higher altitudes, known for their extended flight times and elevated flying levels, were typically utilized for defense roles such as surveillance, data collection, and reconnaissance. Taking advantage of their long-range and ability to operate at great heights, drones in adjacent space were identified as potential tools for early alerts in natural disasters, aiding in emergency situations, and enhancing communication networks. The study also looked into the recent advancements in solar UAVs, highlighting the challenges faced in different operating conditions, especially focusing on the efficiency of solar cells, the functionality of batteries, and the material used for the drone's exterior [23].

In a previous study, the challenges posed by the low-Reynolds number conditions of high-altitude flight on the aerodynamic design, stability, and control of a high altitude, long endurance unmanned air vehicle (HALE UAV) were discussed. The aerodynamic benefits of a flying-wing design made it a compelling choice for such applications and were the focus of the study. The suggested design featured a high-aspect ratio with a swept-wing shape, with the wing's sweep ensuring sufficient leverage for the outer longitudinal and lateral control surfaces. An optimization framework was established in a MATLAB setting, integrating aerodynamics, structural considerations, and stability assessments. To ensure efficient calculations, especially when multiple optimization cycles were involved, low-order analysis tools were used. Specifically, a vortex-lattice technique was employed for wing design aerodynamics, paired with a two-dimensional method for determining airfoil section properties. To predict flow separation limits during design iterations, integral boundary-layer methods were integrated with the panel method. For predicting the wing's weight, a quasi-analytical approach was adjusted for flying-wing designs, and a linear finite-beam element method was applied for the wingbox's structural analysis. Given the challenges of ensuring stability in the thin air of high-altitude flight for flying-wing aircraft, ensuring sufficient directional stability and control was part of the optimization. A modified Genetic Algorithm was the chosen optimization tool. Each of the low-order tools was cross-checked using more advanced methods to ensure their reliability. The study concluded by showcasing the results of using the optimization tools in designing a HALE flying-wing UAV, suggesting its potential as a feasible design choice [24].

in a past study , the capabilities of vertical take-off and landing (VTOL) unmanned aerial vehicles (UAVs) were explored. VTOL UAVs, known for their ability to operate in challenging weather conditions and access remote areas, were highlighted for their unique feature of not requiring a runway. This makes them especially suitable for locations with space constraints and urban settings. However, it was noted that the structural endurance of these UAVs is somewhat limited, particularly for fixed-wing variants. While long-endurance aerial vehicles offer the advantage of sustained flight, their power systems need to harness energy from external sources to adhere to operational standards. A common solution identified was the integration of solar cells onto the UAV wings. The study introduced a tail-sitter VTOL design that incorporated solar cells, emphasizing its potential for extended range and flight duration. Such solar-powered VTOLs were found capable of undertaking longer missions with reduced landing intervals, significantly enhancing their operational performance compared to non-solar counterparts. Computational models considering the inclusion of photovoltaic panels on the UAV structure indicated that VTOLs could potentially double their flight duration around the spring equinox and achieve up to six times longer flight times during the summer solstice [25].

In previous research, an examination of the current development status of various solar-powered unmanned aerial vehicles (UAVs) from both domestic and international perspectives was conducted. From this analysis, the essential technologies required for the design and production of solar-powered UAVs, as well as the current technical challenges, were identified. The study emphasized that as advancements are made in energy system efficiency, innovative aerodynamic design, highly adaptable flight stability and control systems, and the development of efficient propulsion systems, the potential applications for solar-powered UAVs are expected to expand significantly [26].

Other previous research, the growing prominence of Unmanned Aerial Vehicles (UAVs) in reconnaissance activities across various nations was highlighted. One of the primary challenges identified for UAVs was their endurance. Most aircraft traditionally rely on conventional fuels, which not only contribute to pollution but also have limited availability and are costly. This underscored the pressing need to explore alternative, sustainable energy sources. Solar energy emerged as a viable renewable option. The study emphasized the significance of optimizing and designing the aerodynamics of flying vehicles to enhance the utility of UAVs, ensuring they offer effective endurance and reliability, especially at subsonic speeds. This paper introduced a design approach for a solar-powered UAV aimed at achieving extended endurance. Data was gathered, in part, from existing aircraft and UAV systems to support the theoretical calculations for the solar-powered UAV. A comprehensive analysis of past UAVs provided insights into optimal design configurations. The primary goal was to conceptualize a fixed-wing solar UAV with superior endurance. During the initial design phase, the wing geometry and UAV system were crafted using Autodesk Fusion 360 software. A suitable wingspan of 4 meters was determined for the 3-D solar-powered UAV design. Performance metrics were derived from various theoretical parameters. Extensive investigations were conducted to select the most suitable photovoltaic solar cells and battery types for the system, ensuring prolonged endurance. The ultimate aim was to design, analyze, and implement a solar-powered UAV equipped with batteries and solar cells, tailored for long-duration applications [27].

In past research, the quest to enhance the endurance of unmanned aerial vehicles (UAVs) led to the design of a power supply controller capable of automatically switching between solar energy and battery power. This controller was primarily built around an AT89C51 single-chip microcomputer. By measuring the surrounding light intensity and comparing it to a pre-set system threshold, the controller could seamlessly transition the power source for solar UAVs, ensuring a consistent and uninterrupted power supply. The methodology for programming the single-chip microcomputer within the controller was also detailed. The central control mechanism employed Schmidt de shake control for transitioning between solar energy and battery power. The controller's functionalities were evaluated through flight experiments using a small solar-powered UAV. Results indicated that UAVs equipped with this controller could sustain prolonged flights in conditions with fluctuating light intensities. The device showcased commendable performance, in one of past research, the development of a compact, hand-launched, solar-powered unmanned aerial vehicle (UAV) designed for challenging conditions such as low temperatures and high altitudes was discussed. This UAV was envisioned to have the capability for continuous flight, making it ideal for conservation missions targeting rare animals in plateau regions during winter. The study introduced a conceptual design approach for a small solar-powered UAV, tailored for operations in high-altitude, cold environments. An innovative solar irradiance model, sensitive to geographical positioning and time, was incorporated. Taking into account the battery's performance under cold conditions, a weight model for the battery was formulated. The paper further detailed the UAV's design specifics for plateau regions, encompassing layout, structural elements, payload, and avionics. To maximize solar cell coverage, traditional ailerons were omitted, and a singular rudder was employed for both roll and yaw control. Subsequently, a dynamic model for this unique aileron-free UAV layout was established, and the variances in its maneuverability and stability across plateau and plain terrains were examined. Control mechanisms and trajectory tracking systems tailored for the aileron-free UAV were also developed. The culmination of the research was a successful flight test in Qiangtang, Tibet, at an impressive altitude of 4500 m, marking it as China's pioneering solar-powered UAV to operate at such heights in the harsh winter conditions of -30°C. The gathered test data affirmed the effectiveness of the proposed design, the control systems for the aileron-free UAV, and explored the potential for continuous flight with varying payloads based on energy consumption metrics [28].

In past research, the creation of a low-order composite structure module was detailed. This module was designed to craft the wing structure based on specified aerodynamic loads. The wing's structure was divided into non-spar components and spars. Weight estimations for the non-spar elements were derived from empirical formulas, previously employed by NASA for high-altitude, solar-powered UAVs. A distinct numerical method, introduced in the study, was used to size the spar. The spar was conceptualized as a composite rectangular wing-box, believed to bear the entire load without any assistance from other wing components. The necessary laminate layers on each side of the spar were determined iteratively until no potential for failure or buckling was observed. The laminate orientation on each side of the spar drew inspiration from existing high-altitude aircraft structures. To assess the wing-box's deflection under various loads, a linear finite beam element was utilized, with only a quasi-static equilibrium taken into account during the sizing phase. The module was developed in MATLAB, offering the advantage of quick computations, making it suitable for initial design stages or optimization processes. When compared to a high-order commercial software (ANSYS), the module demonstrated remarkable accuracy, with deflection calculations showing less than 0.25% discrepancy. Stress calculations aligned reasonably well with ANSYS, with a maximum deviation of about 4% at peak shear stress levels. Given the typical high safety factors in composite structure design, such a margin of error might be deemed negligible. Additionally, the weight prediction function was cross-referenced with a NASA Pathfinder aircraft, revealing a modest 1.6% variance from the anticipated weight of the studied case [29].

In a previous research, efforts were made to advance the use of renewable energy in Thailand. A small solar-powered unmanned aerial vehicle (UAV) was developed by the team, specifically for environmental monitoring purposes. The study introduced an alternative design for this UAV, targeting a continuous flight duration of 6 hours. The potential of crafting a long-endurance solar-powered UAV for environmental observations was explored. Among various photovoltaic (PV) cells, SunPower C60 mono-crystalline silicon PV cells were chosen for onboard energy conversion. The design process considered varying the wing aspect ratio between 5 and 12, and comparisons were made based on the number of motors to determine the optimal aircraft configuration. Findings indicated that a hybrid solar-powered UAV weighing 5.5 kilograms could potentially achieve a 6-hour continuous flight from 9AM to 3PM under Thailand's climatic conditions. This UAV, with a wingspan of 4.06 meters, was designed to produce a minimum electrical output of 100 Watts. It was equipped with two brushless electric motors, allowing it to maintain a cruising speed of 8 meters per second, withstand wind speeds up to 5 meters per second, and attain altitudes up to 1 kilometer above sea level, fulfilling its environmental monitoring role [30].

In past research, the creation of a low-order composite structure module was detailed. This module was designed to craft the wing structure based on specified aerodynamic loads. The wing's structure was divided into non-spar components and spars. Weight estimations for the non-spar elements were derived from empirical formulas, previously employed by NASA for high-altitude, solar-powered UAVs. A distinct numerical method, introduced in the study, was used to size the spar. The spar was conceptualized as a composite rectangular wing-box, believed to bear the entire load without any assistance from other wing components. The necessary laminate layers on each side of the spar were determined iteratively until no potential for failure or buckling was observed. The laminate orientation on each side of the spar drew inspiration from existing high-altitude aircraft structures. To assess the wing-box's deflection under various loads, a linear finite beam element was utilized, with only a quasi-static equilibrium taken into account during the sizing phase. The module was developed in MATLAB, offering the advantage of quick computations, making it suitable for initial design stages or optimization processes. When compared to a high-order commercial software (ANSYS), the module demonstrated remarkable accuracy, with deflection calculations showing less than 0.25% discrepancy. Stress calculations aligned reasonably well with ANSYS, with a maximum deviation of about 4% at peak shear stress levels. Given the typical high safety factors in composite structure design, such a margin of error might be deemed negligible. Additionally, the weight prediction function was cross-referenced with a NASA Pathfinder aircraft, revealing a modest 1.6% variance from the anticipated weight of the studied case [31].

In a past paper, the development journey of AtlantikSolar was discussed. This is a lightweight, 6.9 kg, hand-launchable, low-altitude solar-powered unmanned aerial vehicle (UAV) that has achieved an 81-hour continuous flight, setting a new endurance record for aircrafts under 50 kg. The primary objective was to enhance the reliability of such solar-powered UAVs, especially in challenging weather conditions like cloud cover or high winds. Energetic system models and a design methodology were introduced, and these were incorporated into a publicly accessible design framework tailored for solar-powered UAVs capable of perpetual flight. The AtlantikSolar UAV was then used as a practical example, detailing its specific features. The development of its airframe, avionics, hardware, state estimation, and control methods for autonomous operations were elaborated upon. Flight data from the UAV was utilized to validate the design framework. The 81-hour flight, covering a ground distance of 2,338 km, showcased AtlantikSolar's impressive performance metrics, surpassing previous solar-powered UAVs. The UAV's capabilities were further highlighted, indicating its potential for continuous flight during a 6-month period around June 21 in mid-European regions. Additionally, it was noted that the UAV could undertake multi-day flights carrying small optical or infrared cameras. This performance is considered the pinnacle in current solar-powered low-altitude perpetual flight capabilities. The study wrapped up by sharing insights from the three-year development journey of AtlantikSolar and pinpointing areas where future advancements in solar-powered UAVs could be made [32].

In a past study, the integration of emerging energy sources, such as solar and hydrogen energy, into Unmanned Aerial Vehicles (UAVs) was explored. These energy sources were considered for hybrid power systems, addressing the UAV's needs for miniaturization, lightweight structures, and environmental considerations. The shift towards hybrid electrical propulsion in UAVs emphasized the evolution towards Hybrid-Powered Systems (HPS). To achieve extended flight durations and enhance UAV energy efficiency, significant attention was directed towards the Energy Management Strategy (EMS) of the HPS. This involved digital simulations, ground demonstrations, and select flight tests. Central to the EMS is the control algorithm, either off-line or on-line, which optimizes the dynamic electrical power distribution, influencing the efficiency and fuel economy of the onboard hybrid-powered system. This paper provided an overview of optimal energy management strategies for UAVs. It began by outlining the features of typical new energy sources used in UAVs, followed by an analysis of hybrid power system architectures. Given the backdrop of these energy sources and system configurations, a detailed comparison of current EMS approaches was presented. The analysis weighed the real-time capabilities, computational demands, and optimization performance of these strategies, considering the UAV's optimal control and operational modes. The study concluded by projecting the future directions and challenges of applying energy management strategies to UAVs [33].

In a past scientific paper, the exploration of possibility-based multidisciplinary optimization for the design of electric-powered unmanned aerial vehicles (UAVs) was discussed. An integrated UAV (iUAV) analysis tool tailored for electric-powered motors was introduced and its accuracy was confirmed using a configuration similar to Predator A, focusing on aerodynamics, weight, and performance metrics. Instead of traditional piston engines and fuel, the introduction of an electric motor, power controllers, and batteries was suggested from an eco-friendly perspective. Additionally, the development of an in-house Possibility-Based Design Optimization (iPBDO) tool was highlighted, designed to manage uncertain variables and parameters, and to shift constraints to ensure feasible design spaces. To streamline the iPBDO process, a sensitivity analysis was conducted, aiming to minimize the number of design variables and computational demands. The primary goal was to enhance the endurance of the electric-powered UAV. Results from the iPBDO indicated that this approach, though more conservative, provided more reliable UAV configuration outcomes compared to conventional deterministic optimization methods. The efficacy of this method was further showcased through a high-fidelity analysis, which validated the optimal configurations of the electric-powered UAV at two distinct possibility index values and a baseline [34].

In a previous study, the benefits of Unmanned Aerial Vehicles (UAV) over traditional manned aircraft were discussed. The diverse applications of UAVs were highlighted, with a particular emphasis on the significance of extended flight endurance, which can be augmented through the incorporation of photovoltaic cells. A concise historical perspective on the evolution of solar-powered UAV designs was provided, noting the past challenges and the advancements needed in UAV components to realize a viable project, challenges that are now surmountable. The primary elements of a solar-powered UAV structure and the essential principle of energy balance, crucial during the design and operation phases of such UAVs, were elucidated. A method to gauge the potential increase in flight endurance of an electric UAV equipped with photovoltaic cells was introduced. This method was applied to a pilot project and demonstrated precision when juxtaposed with an experimental scenario. The primary objective of this method was to aid in evaluating the potential enhancement in electric UAV flight duration due to the integration of a photovoltaic system before embarking on experimental trials [35].

In prior study, the development of an affordable flight control system for a small, hand-launched, solar-powered, aileron-less unmanned aerial vehicle (UAV) was detailed. To enhance the precision of the entire system model and to measure the impact of individual subsystems, meticulous modeling of the UAV's energy and control system was undertaken. This modeling incorporated elements like a solar model, engine, energy storage, sensors, state estimation, control law, and actuator module, all grounded in experimental data and foundational principles. A comprehensive system simulation, integrated with a 6 degree-of-freedom (DOF) model, was crafted based on a standard mission path, yielding insights into parameter accuracy and energy equilibrium. Subsequently, a hardware-in-the-loop (HIL) experimental approach anchored in the Stewart platform (SP) was introduced. This approach encompassed three modes: acceleration, angular velocity, and attitude, aiming to validate the control system across various flight envelope states. The overarching system design was then assessed through flight tests at diverse altitudes. These tests facilitated the refinement of aerodynamic force coefficients and sensor inaccuracies using actual flight data. It was observed that as altitude increased, cruise power ranged from 47 W to 78 W, trajectory tracking accuracy varied between 23 m and 44 m, and while sensor measurement noise amplified, the bias diminished [36].

Prior work elucidated an optimization-centric design paradigm for solar-powered unmanned aerial vehicles, emphasizing holistic improvements by scrutinizing interdependent subsystems. Constructing upon existing methods, the presented approach tailors key propulsion targets that directly influence routing algorithms. Subsequently, encompassing known mission specifications of such vehicles and factoring critical design variables like wing geometry and scheduled operation, an integrated optimization procedure is executed, radically reducing integrated airframe mass. Methodical evaluation quantifies wing architectural selections against optimization products, validating pronounced mass diminutions. Consolidating findings evinces markedly enhanced energy storage requisites when preferentially optimizing propulsion systems, translating to appreciable vehicle mass deductions [37].

One of past research, the potential of near-space solar-powered unmanned aerial vehicles (UAVs) was recognized due to their ability to perform at high altitudes for extended durations. The concept of deploying these UAVs into near-space using a balloon-borne method was introduced, highlighting its superiority in swiftly and safely navigating through turbulent zones compared to conventional take-off techniques. The focus of this study was on the control mechanisms associated with balloon-borne launching for such UAVs. The motion during the launch process was categorized into longitudinal and lateral directions, with an in-depth exploration of the longitudinal motion and its governing equations. The necessary flight states and conditions that the UAV should adhere to during this phase were also delineated. Subsequently, the study identified target variables and constraints to frame the optimization challenge. An approach using control variable parameterization was employed to determine the optimal pitch angle during the release and ascent phases. A comprehensive three-channel attitude stabilization controller was then crafted: the longitudinal channel utilized the optimal pitch angle as guidance, the lateral channel aimed for zero inclination angle control, and the course channel focused on stabilization. Simulation outcomes demonstrated that the proposed control strategy effectively transitioned the UAV from a vertical position to a horizontal cruising flight. Key parameters like angle of attack, peak speed, and maximum axial acceleration during the ascent remained within the predefined limits [38].

In past research, the diverse applications of unmanned aerial vehicles (UAVs) were explored, encompassing areas such as military operations, reconnaissance, disaster response, communication support, geographical assessments, and photography. The growing integration of UAVs into daily activities was noted. However, a prevalent limitation identified was their restricted endurance. It was observed that the majority of UAVs rely on traditional fuels for both propulsion and the operation of onboard systems. Given the size constraints of these UAVs, their fuel capacity inherently curtails their operational duration. This highlighted an imperative for alternative solutions to not only extend their endurance but also to mitigate environmental impacts. With Sub-Saharan Africa receiving ample solar radiation, the potential for solar-powered UAVs to achieve optimal flight performance in this region was emphasized. Thus, the study aimed to shed light on the potential benefits and feasibility of deploying solar-powered UAVs in Sub-Saharan Africa to harness maximum flight efficiency [39].

In a previous paper, the potential of AtlantikSolar, a compact, hand-launchable, solar-powered fixed-wing unmanned aerial vehicle, was explored for its capacity to support extended autonomous aerial sensing and mapping tasks. The design of the platform and the integrated state estimation, control, and path-planning mechanisms were examined. A multifaceted sensor payload was introduced, encompassing a multi-camera system, enhanced onboard processing, and a robust communication link to the ground. The research included comprehensive field tests, which encompassed public demonstrations for search-and-rescue missions and prolonged mapping tasks. Analysis from the study indicated that AtlantikSolar is capable of operating throughout daylight hours and boasts a baseline flight endurance of at least 8 hours annually when equipped with its complete multi-camera mapping system. Accompanying the study is the release of an open dataset, offering both raw and processed data [40].

In past study, the resource allocation design for multicarrier (MC) systems utilizing a solar-powered unmanned aerial vehicle (UAV) to deliver communication services to multiple downlink users was examined. The combined design of the UAV's three-dimensional positioning and the allocation of power and subcarriers was studied with the aim of maximizing the overall system throughput. This design challenge was characterized as a mixed-integer non-convex optimization problem, which, if approached directly, would demand an overwhelming computational effort to discern the optimal solution. Consequently, a more manageable suboptimal iterative method, grounded in successive convex approximation, was introduced. Simulations demonstrated that this proposed approach significantly outperformed several standard methods in terms of system throughput [41].

In a past paper, a method for 3D path planning of solar-powered UAVs targeting fixed points and tracking solar energy was explored. The challenge identified was managing the interplay between UAV movement, mission requirements, energy generation, and consumption when continuously monitoring fixed targets. The proposed solution was to plan the UAV's flight paths on a virtual cylindrical surface in 3D space, centered around the fixed target. To achieve this, the UAV's motion was redefined, and its movement characteristics and forces were analyzed based on this new model. Following this, the state variables at each waypoint were parameterized using optimization variables and their derivatives, incorporating a thrice-introduced spline interpolation function to deduce these derivatives. To streamline the optimization process, the UAV's horizontal speed component was set to its minimum power flight speed, its yaw rate was fixed, and the sun's position was assumed constant over short durations. Simulations indicated that, unlike UAVs maintaining a constant altitude, the UAV in this study would adjust its altitude to optimize its attitude for maximum energy generation [42].

In a past paper, the focus was on examining the resource distribution method for multicarrier solar-powered UAV communication systems. The study concentrated on a solar-powered UAV, aimed at providing sustainable communication to ground users. It delved into the joint design of the UAV's three-dimensional flight path and the allocation of wireless resources, targeting to boost the total system output over a set time frame. Initially, the evaluation involved an offline resource allocation plan, which operated on the premise of predetermined channel gain knowledge. This approach presented a complex optimization problem, factoring in elements like aerodynamic power usage, solar energy harvesting, limited energy storage capacity, and user service quality requirements. Despite the complexity, an optimal solution was reached through monotonic optimization, identifying the most efficient 3D flight path and power/subcarrier distribution. The study then transitioned to designing an online algorithm, requiring real-time and statistical data on channel gains. While this optimal online approach was informed by the offline strategy and demanded extensive computational resources, a less demanding iterative suboptimal online method was also proposed, utilizing successive convex approximation. Simulation results demonstrated that the online strategies closely matched the offline benchmark in performance and markedly outperformed two basic methods. The study also underlined the trade-off between harvesting solar energy and maintaining energy-efficient communication, noting the UAV's initial rise to higher altitudes for better solar collection followed by descent to reduce communication path loss with users [43].

In previous research, the comprehensive design, creation, and validation of MARAAL, a solar-powered UAV intended for day-night operations in subtropical regions at low altitudes, was explored. This SUAV, developed at the Unmanned Aerial Laboratory of IIT Kanpur, was characterized by a 5.35m wingspan, a maximum endurance of 18 hours, and the capacity to carry up to 6kg of payload. The conceptual design approach, accompanied by simulation outcomes, was presented. Additionally, the process of solar cell integration was elaborated upon. Emphasis was also placed on the construction methodologies and the specifics of the onboard electronics and surveillance tools [44].

In previous research, the challenge of achieving perpetual flight for solar-powered UAVs (SPUAVs) in middle and high latitude regions during winter was addressed. Due to the constraints of low sun elevation angle and limited daylight hours, obtaining adequate solar energy becomes a significant challenge. The potential of sun-tracking through the modification of wing geometry and adjusting flight direction was explored as a viable solution to harness more solar energy. The focus of the study was on the energy optimization method for a Z-shaped sun-tracking morphing-wing SPUAV. When compared to the traditional planar wing, it was determined that the optimal Z-shaped wing could achieve extended flight endurance, especially in middle and high latitude regions during winter. Furthermore, the study revealed that as the conversion efficiency of solar cells increased, the Z-shaped wing was even more effective in energy collection. This design, in conjunction with the proposed energy optimization method, offers promising avenues for enhancing the flight endurance and expanding the perpetual flight latitude of SPUAVs [45].

3. METHODOLOGY

This chapter has been divided into several sections. The first section will deal with general information about aerodynamics science and related equations, and the second section will deal with general information about Solar power and Solar cells design. The actual work will start from the third section, a model of the aircraft, the MQ-9, will be selected, and the development of its flight range will be studied by adding solar panels placed on the vehicle's wing. It will be drawn using the CAD program, Placing the solar panels on the wing and discussing the results.

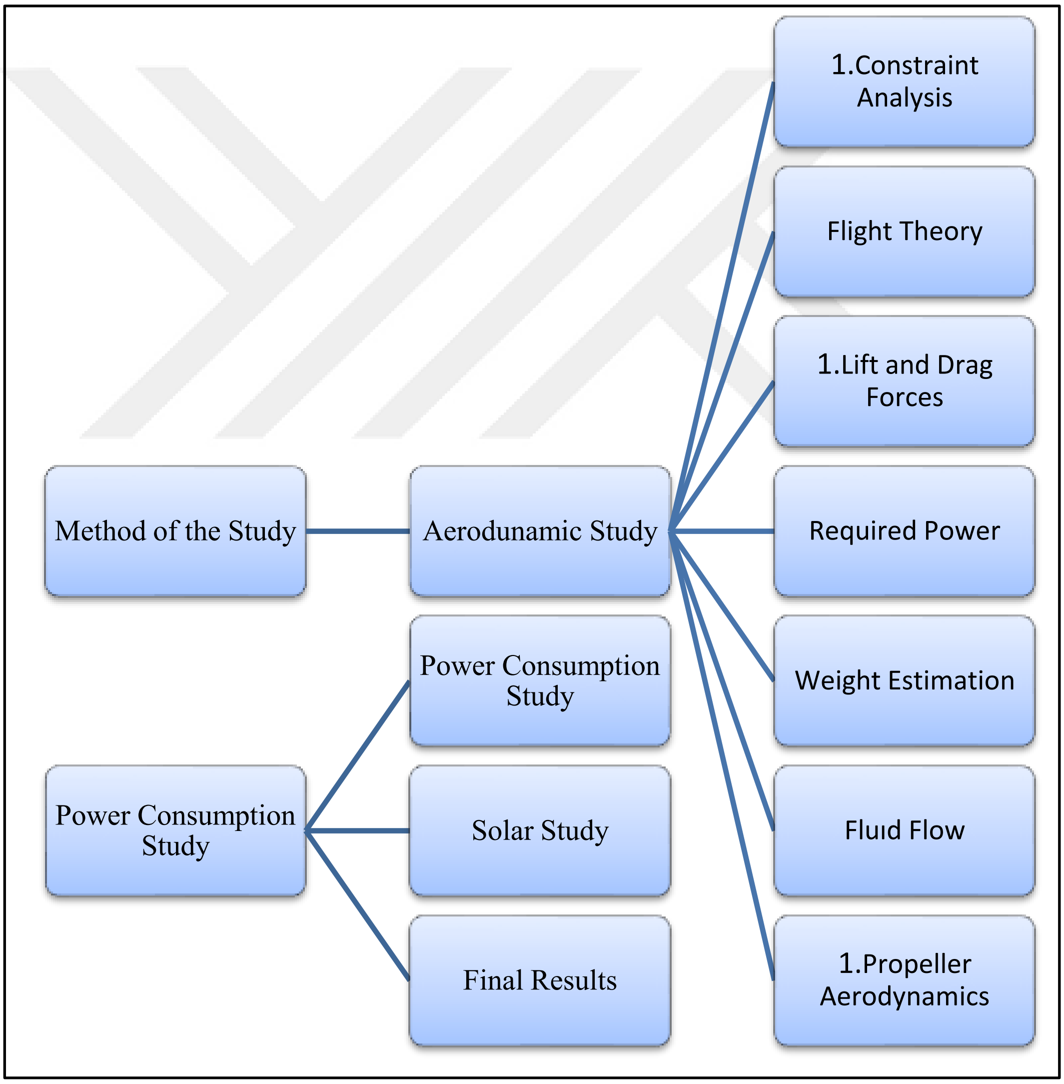

Figure 3.1: Methodology Overview: Aerodynamics and Energy Studies.

3.1 BACKGROUND OF AERODYNAMIC STUDY

In this study we will be talking briefly about the aerodynamic study of unmanned aerial vehicle and specially of the MQ9 UAV, sometimes called Predator B is capable of remotely controlled or autonomous flight operations, developed by General Atomics Aeronautical Systems, designed for long-endurance, high-altitude surveillance, our model has overall dimensions like the following, Wingspan equal to $20\ m$ and $11\ m$ in Length and $3.8\ m$ in height and its weight is equal to $2223\ kg$ and has $712\ kW$ turboprop engine and its range is up to $1850\ km$ and operational altitude at $15000\ m$.

Figure 3.2: MQ-9 UAV.

3.1.1 Constraint Analysis

The design of UAV has several constrains like the UAV must take-off on short runways where take-off distance should not exceed $1.5\ km$ and should consume the least amount of energy with maximum payload equal to $1700\ kg$ in addition to minimize manufacturing costs as much as possible, so the constraint analysis is the first step of our design.

Table 3.1: General Characteristics Of MQ-9.

General characteristics	
Length [m]	11
Wingspan [m]	20
Height [m]	3.8
Maximum Payload [kg] – Endurance [h]	1700 kg – 27 h
Power Plant [kw]	671
Maximum Speed [km/h]	482
Range [m]	1850
Operational Altitude [m]	7500

3.1.2 Flight Theory

The UAV must adhere to the same aerodynamic principles as conventional aircraft. Prior to conducting any aerodynamic analysis, it is crucial to consider the atmospheric conditions, providing insight into potential challenges for the solar-powered unmanned aerial vehicle (SPUAV). The aircraft's performance is directly influenced by the altitude at which it operates. Notably, within the altitude range of $10\ km - 23\ km$, the air temperature remains relatively constant at around $-50°C$. Wind speeds need to be defined as a function of altitude. It is essential to specify the wind speed that the SPUAV may encounter at its maximum and minimum altitudes. The air specifications at various altitudes are detailed in Table 3.2, which outlines air parameters at different altitudes [41].

Table 3.2: Air Parameters at Different Altitudes.

Altitude according to sea level [km]	**Temperature** [$°c$]	**Absolute Pressure** $10^4 N/m^2$	**Density** kg/m^3	**Wind speed at 90% wind** m/s
0.0	15.00	10.13	1.789	0
2	2	7.950	1.726	13
4	-10.98	6.166	1.661	17

Table 3.2: Air Parameters at Different Altitudes. " Table Continued ".

7	-30.45	4.111	1.561	21
8	-36.94	3.565	1.527	22
10	-49.90	2.650	1.458	24
15	-56.50	1.211	1.422	45
25	-51.60	0.2549	1.448	10

3.1.3 Lift and Drag Forces

Figure 3.2 below shows a basic free body diagram of the forces exerted onto an aircraft during flight. For level equilibrium flight it can be assumed that:

$$W = L \quad \& \quad T = D \tag{3.1}$$

Respectively the lift and drag forces can be expressed by,

$$L_{force} = \frac{1}{2}\rho V^2 S C_L \quad \Rightarrow \quad C_L = \frac{2L_{force}}{\rho V^2 S} \tag{3.2}$$

$$D_{force} = \frac{1}{2}\rho V^2 S C_D \quad \Rightarrow \quad C_D = \frac{2D_{force}}{\rho V^2 S} \tag{3.3}$$

Were, The lift coefficient C_L and drag coefficient C_D are dimensionless values that quantify the lift and drag forces experienced by a body in a fluid environment, respectively. These coefficients are influenced by the surface area S of the object, expressed in square meters, the velocity V of the object through the fluid, measured in meters per second, and the fluid's density ρ, measured in kilograms per cubic meter. These values are critical in aerodynamic calculations for predicting how objects will behave when subjected to fluid forces.

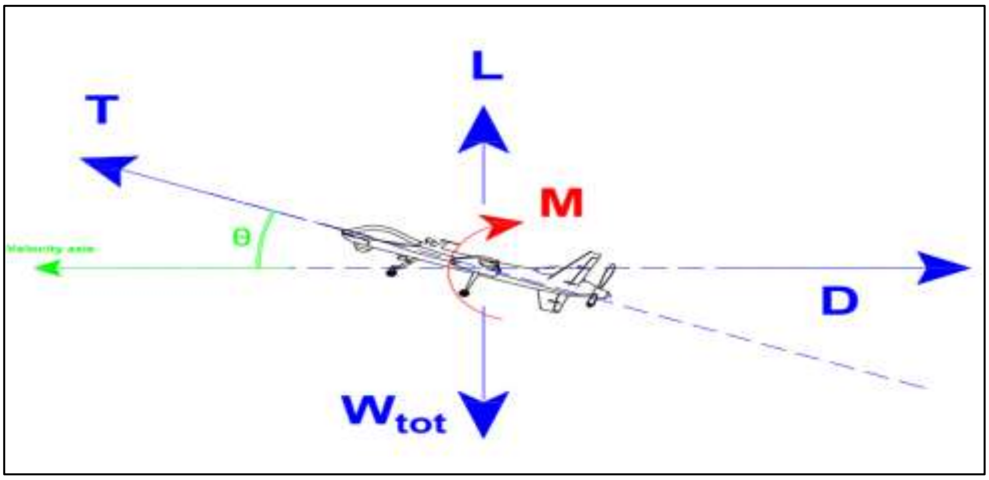

Figure 3.3: Aerodynamic Forces on Free Body Diagram.

The vector sum of forces along the Vertical axis equals zero:

$$W - T\sin\theta - L = 0 \tag{3.4}$$

The vector sum of forces along the Horizontal axis equals zero:

$$T\,cos\theta - D = 0 \tag{3.5}$$

In steady level flight, it is necessary for the pitching moment to be zero:

$$M = 0 \tag{3.6}$$

The angle θ is very small so that we can consider the following:

$$T = D \tag{3.7}$$

$$L = W \tag{3.8}$$

Eq 3.7 and Eq 3.8 present steady state level flight as the following:

a. The lift must be equal to the weight of the aircraft.

b. The Drag and Thrust should be equal.

c. The aerodynamic pitching moment should be zero.

3.1.4 The Stall Speed

The stall speed $[m/s]$can be found when the lift coefficient is at its maximum value like the following.

$$V_{Stall} = \sqrt{\frac{2W}{\rho V^2 S\, C_L}} \tag{3.9}$$

3.1.5 The Required Power

The power needed for consistent level flight is determined by the key relationship between thrust and power. In such flight conditions, the power needed is the thrust required multiplied by the aircraft's airspeed. Therefore, the formula to calculate power for steady level flight involves multiplying the drag coefficient by the airspeed of the aircraft.

$$PW = D.V \tag{3.10}$$

The available power at the propeller, drives the UAV, with power supplied by an electric motor. This electric motor, operating on electromagnetic principles, relies on batteries for its power source, making the battery a pivotal element in determining aircraft performance. The power available to the propeller is established by the manufacturer through the power rating and associated information. The efficiency of the motor also plays a crucial role in determining the actual power available for propulsion. For MQ-9 the available power is $671\ kw$ that is given by the UAV's Motor taking in consideration the losts and efficiency of the system components.

3.1.6 Maximum speed

The maximum power output of an engine serves as a constraint on the achievable air speeds that an aircraft can maintain in steady level flight. Specifically, when the engine operates at full throttle, the power required for steady level flight equals the maximum power capacity of the engine. The lowest attainable velocity for an aircraft is represented by the stall velocity. Graphically, the maximum velocity is determined by the intersection of the power available, and power required curves. For MQ-9 the maximum speed is $482\frac{km}{h}\ equal\ to\ 260\ knots.$

3.1.7 SPUAV Weight Estimation

Empirical equations were developed to estimate weight during the early design stages. In the process of aerofoil selection, the most critical considerations revolve around stall speed and take-off distance, necessitating the use of aerofoils with high Cl_{MAX} and superior lift characteristics. Consequently, rigorous testing is imperative to ensure optimal performance under these conditions. Wing sizing, guided by constraint analysis, leads to the design of a minimum wing area that fulfils all constraints. This minimum design point is chosen after evaluating parameters such as take-off distance, stall speed, rate of climb, cruising speed, and turning speed. Additionally, special attention is given to designing an effective wingtip to mitigate excessive induced drag, thereby enhancing the overall performance of the power plant. The horizontal tail's role is to balance the moments generated by both the wing and fuselage. In this context, the primary objective is to craft an efficient tail that strikes a balance between size and weight, ensuring it can effectively fulfil its responsibility. After initial calculations, the design of the vertical tail is geared towards maintaining both directional stability and meeting the requirements for safe landings [46].

The total weight of the UAV is the sum of the system component as following.

$$W_{total} = W_{Struct} W_{Solar} W_{Battery} W_{Prop} W_{Manager} W_{Avionics} W_{Payload} \qquad (3.11)$$

Were,

The system's total weight, captured by W total , integrates the weight of various components. These include W Struct , the structural weight; W Solar, associated with the solar cells; W Battery, for the energy storage batteries; W Prop , which is the propulsion system's weight; W Manager , the weight of the energy management system; W Avionics , representing the avionics weight; and W Payload , the weight of the mission's payload, which can reach up to 1700 kg at its maximum. Each weight parameter is pivotal, affecting the overall mass and the system's performance criteria.

The structural weight is estimated parametrically, where it is considered a function of the number of boom tails (N), reference area (S), and aspect ratio (AR).

$$W_{Struct} = 8.763\ N^{0.311}\ S^{0.778}\ AR^{0.467} \qquad (3.12)$$

The solar panels are electrically linked together and sandwiched between two layers of non-reflective, clear material. As a result, the total weight calculation of the solar panel should include both the weight of the cells and the protective layers. This concept is encapsulated in a specific formula, where k_{Solar} is defined as the combined surface density of both the solar cells and their encapsulation, and S_{Solar} denotes the total surface area that the solar cells occupy.

$$W_{Solar} = k_{Solar} S_{Solar} \tag{3.13}$$

Regarding the battery, its weight is directly related to the energy it needs to store ($Q_{Battery}$) and inversely related to its weight-energy ratio ($k_{Battery}$).

$$W_{Battery} = k_{Battery} Q_{Battery} \tag{3.14}$$

The propulsion system comprises four components: control electronics, motor, gearbox, and propeller. Based on previous solar-powered aircraft designs, it is assumed that the weight of these four components exhibits a linear relationship with power output. Additionally, each part has its power densities and efficiencies. To maintain consistency within the system, the maximum continuous power input of the motor, denoted as $P_{Max.prop}$, is taken into consideration. A constant, k_{Prop}, is utilized to estimate the weight of the entire propulsion system.

$$W_{Prop} = k_{Prop} P_{Max.prop} \tag{3.15}$$

The energy manager serves two primary purposes. Firstly, it adjusts the voltage of the solar cells to maximize their power output. Secondly, it optimizes the voltage and current output to various subsystems, including the propulsion system and avionics. Depending on the system's application, the weight is directly proportional to the maximum power, with a ratio denoted as $k_{Manager}$. The maximum power of the system is directly determined by the maximum power output of the solar cells, referred to as $P_{Max.Solar}$.

$$W_{Manager} = k_{Manager}\, P_{MaxSolar} \tag{3.16}$$

The weight of the avionics and payload remains constant and is not influenced by the size or power of other systems. These weights are determined at the outset of the design and remain unchanged throughout [47].

For MQ-9 the total weight of the UAV without the solar system components is $2223\ kg$ and with maximum payload is equal to $4760\ kg$.

3.1.8 Fluid Flow Around UAV Body

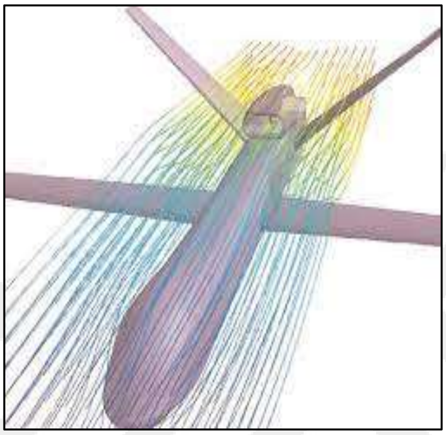

Figure 3.4: Air Flow Around Airplane Body.

Aerodynamics is the study of fluid flow, with a specific emphasis on air in this discipline, as reflected in its name. Through the application of aerodynamics, the correlation between airflow and the forces acting on the object under examination becomes evident. Notably, among the prominent forces to be discussed later are drag forces and lift forces. Understanding the types of airflow is crucial in the study of aerodynamics, with two primary classifications being turbulent flow and laminar flow. Turbulent flow is characterized by irregular and chaotic air movement. In contrast, laminar flow is smooth and gentle along surfaces [55]. The flow pattern can transition, for instance, from laminar to turbulent, as illustrated in the figure below, starting on an aircraft wing.

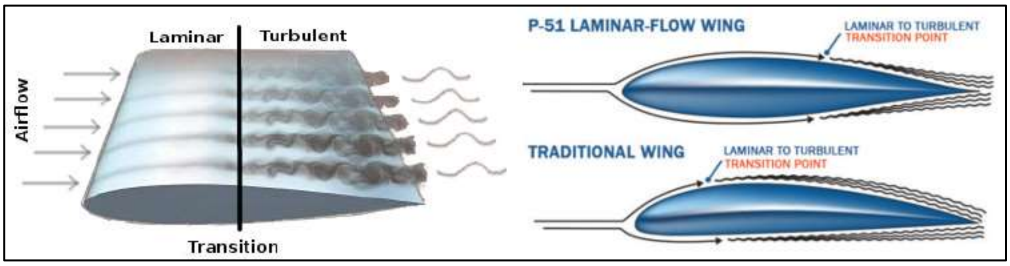

Figure 3.5: Airflow Transit From Laminar to Turbulent Flow on the Wing.

Various methods and techniques are employed to investigate aerodynamics in both airborne and ground-based vehicles. Physical equations, including the Navier-Stokes equations, the Bernoulli equation, and viscous fluid flow equations, are utilized in this study. Computer-based approaches, such as Computational Fluid Dynamics (CFD), which relies on finite element methods, are also common. ANSYS Fluent is a notable software extensively used for CFD simulations in the realm of aerodynamics.

3.1.9 Bernoulli And Navier-Stokes Equations

The primary equations frequently employed in aerodynamics studies are the Bernoulli equation and the Navier-Stokes equations. According to Bernoulli's principle, a decrease in fluid pressure or potential energy correlates with an increase in its velocity [45]. The following equation elucidates the Bernoulli equation and its associated variables [46].

$$p + 0.5 \times \rho \times v^2 = constant \tag{3.17}$$

Were,

p: Fluid pressure $[Mpa]$

ρ: Fluid density $[kg/m3]$

v: Fluid velocity $[\mathrm{m}/s]$

In aviation applications and aerodynamic analysis, these equations play a crucial role in calculating the lift force on an airfoil. If the airflow on the lower surface of the wing has a lower velocity than the upper surface, it indicates that the pressure on the upper surface of the wing will be lower than on the lower surface [45].

The Navier-Stokes equations are instrumental in describing fluid flow and the forces acting on it. These equations provide a comprehensive representation of fluid movement, encompassing variables such as speed, pressure, temperature, and more. They are employed to analyze the motion of both conventional and unmanned aircraft under diverse weather conditions, including turbulence, wind, and other external forces [47]. The Navier-Stokes equations consist of three components: the momentum equation, the continuity of mass, and the energy equation [48].

a. Continuity equation (Conservation of mass)

$$\frac{\partial u}{\partial x} + \frac{\partial v}{\partial y} + \frac{\partial w}{\partial z} = 0 \tag{3.18}$$

Were,

x, y, z: Directions

u: Velocity component in the x-direction $[m/s]$

v: Velocity component in the y-dirction $[m/s]$

w: Velocity component in the z-dirction $[m/s]$

b. Momentum equation

$$\frac{\partial u}{\partial t} + u \times \frac{\partial u}{\partial x} + \mu \times \frac{\partial u}{\partial y} + w \times \frac{\partial u}{\partial z} = -\left(\frac{1}{\rho}\right) \times \frac{\partial p}{\partial x} + \mu \times \left(\frac{\partial^2 u}{\partial x^2} + \frac{\partial^2 u}{\partial y^2} + \frac{\partial^2 u}{\partial z^2}\right) \tag{3.19}$$

Were,

t: Time $[s]$

p: Pressure of the fluid [Mpa]

ρ: Density of the fluid $[kg/m3]$

μ: Kinematic viscosity $[m^2/s]$

c. Energy equation

$$\frac{\partial T}{\partial t} + u \times \frac{\partial T}{\partial x} + v \times \frac{\partial T}{\partial y} + w \times \frac{\partial T}{\partial z} = -\left(\frac{1}{\rho \times Cp}\right) \times \left(u \times \frac{\partial T}{\partial x} + v \times \frac{\partial T}{\partial y} + w \times \frac{\partial T}{\partial z}\right) + \left(\frac{k}{\rho} \times Cp\right) \times \left(\frac{\partial^2 T}{\partial x^2} + \frac{\partial^2 T}{\partial y^2} + \frac{\partial^2 T}{\partial z^2}\right) + \varepsilon \tag{3.20}$$

Were,

T: Temperature $[K]$

Cp: Specific heat at constant pressure $[J \cdot kg^{-1} \cdot K^{-1}]$

k : Thermal conductivity $[W \cdot m^{-1} \cdot K^{-1}]$

ε: Internal energy dissipation $[J]$

3.1.10 Propeller Aerodynamics

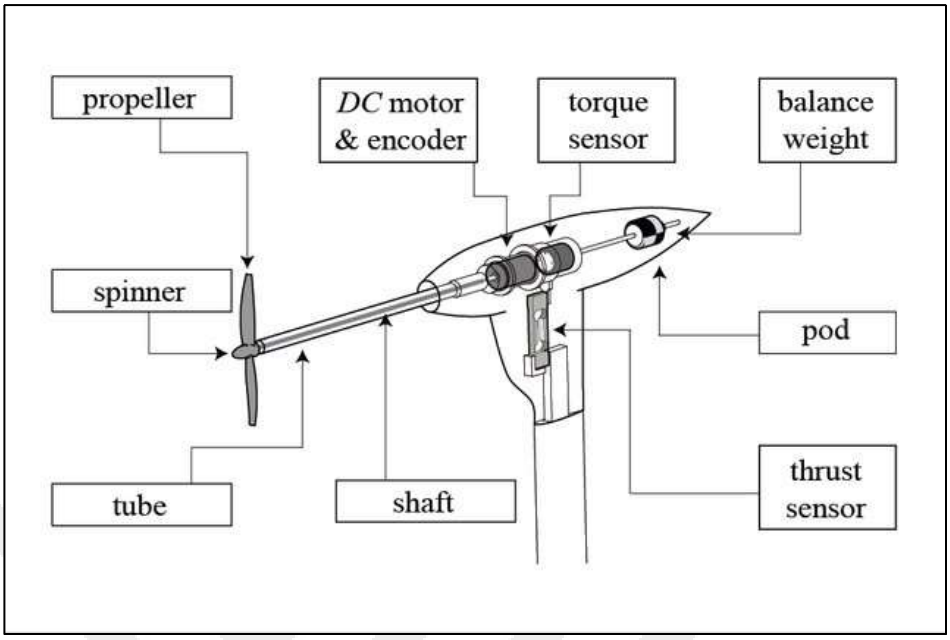

Figure 3.6: Propeller Connection to UAV.

In the case of a propeller, it is assumed that there exists a specific point at a radius "r" on the propeller where the blade element efficiency matches that of the entire propeller. As a result, the performance of the entire propeller is represented by the blade element at that particular point. This straightforward evaluation method of a propeller is referred to as the Simple Blade Element theory (SBE).

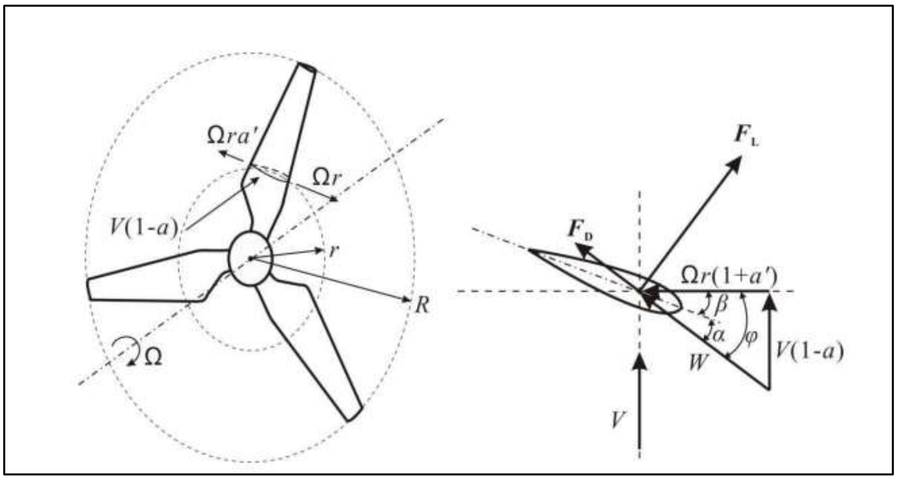

Figure 3.7: Propeller Forces and Angles.

The angle between the incoming airflow and the rotating plane is determined as follows:

$$tan\emptyset = \frac{V}{\omega\, r} \tag{3.21}$$

Where x is the angular velocity of the propeller, and $x = 2pn$, n is the propeller rotation speed, the velocity of incoming flow is V. Take the advance ratio $J = V/nD$ to the formula, it has.

$$tan\emptyset = \frac{J}{\pi\, k} \tag{3.22}$$

Were,

In the context of propeller design, D represents the diameter, which is a fundamental dimension determining the size of the propeller. The relative position along this diameter is expressed through K, defined as k=2r/D, where r is the radial distance from the centre of the propeller. The lift coefficient for a blade element is denoted as C_{Lp}, which is a key factor in calculating the lift force that the propeller blade generates. Similarly, C_D represents the drag coefficient, indicating the resistance encountered by the blade element as it moves through the air or fluid. These coefficients are essential for analyzing the aerodynamic performance of the propeller blades.

These coefficients can be calculated using the aerodynamic model previously applied for aircraft. The drag-lift angle of the propeller blade is denoted as γ:

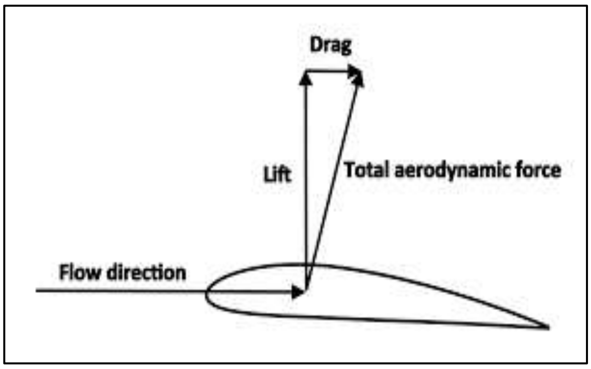

Figure 3.8: Lift-Drag Angle.

$$\gamma = C_{Dp}/C_{Lp} \tag{3.23}$$

The reference area of the propeller is typically defined as the disk area swept by the rotating blades. and is used in various aerodynamic calculations and performance analyses for propellers. Here its S_p, so the thrust of the propeller is:

$$T = 1/2.\rho V_h^2\, S_p\, (C_{Lp}\ \cos\emptyset - C_{Dp}\ \sin\emptyset\ ) \tag{3.24}$$

$$V_h = \sqrt{V^2 + (\pi nkD)^2} \tag{3.25}$$

ρ is the local air density and V_h is the airflow velocity which relative the propeller blade, and Based on Eqs.3.18 and 3.21, the thrust of the propeller is:

$$T = 1/2.C_{Lp}\ \rho V^2\ S_p \sqrt{(1+\cot\hat{}2\,\emptyset\,)\ (\cot\emptyset - \tan\gamma)} \tag{3.26}$$

Correspondingly, the circumferential force of the propeller, there is:

$$R = 1/2.C_{Lp}\ \rho V^2\ S_p \sqrt{1+\cot^2\emptyset}\,(1+\tan\gamma.\cot\emptyset) \tag{3.27}$$

The efficiency of the propeller is as follows [47]

$$\eta_{prop} = \frac{TV}{Rn\pi kD} = \tan\emptyset.\frac{\cot\emptyset - \tan\gamma}{1+\tan\gamma.\cot\emptyset} = \frac{tan\emptyset}{\tan(\emptyset+\gamma)} \tag{3.28}$$

3.1.11 Flight Dynamics

The aircraft will undergo three distinct flight stages: climb, level flight, and descent. The force analysis for each of these stages is described as follows.:

$$\begin{cases} L = G.\cos\theta \\ T = D + G.\sin\theta \end{cases} \qquad Climb \tag{3.29}$$

$$\begin{cases} L = G \\ T = D \end{cases} \qquad Flat \tag{3.30}$$

$$\begin{cases} L = G.\cos\theta \\ D = T + G.\sin\theta \end{cases} \qquad Descent \tag{3.31}$$

Here, h represents the trail angle of the aircraft, and $L, D, T\ and\ G$ denote the lift, drag, thrust, and gravity forces, respectively. Eq 3.29 through Eq 3.31 can be combined into a dimensionless coefficient equation as follows:

$$\sqrt{C_L^2 + (C_T - C_D)} = C_R \tag{3.32}$$

In the provided equation, CL and CD represent the lift coefficient and drag coefficient of the Solar Powered Unmanned Aerial Vehicle (SPUAV). CR signifies the gravity coefficient of the aircraft.

$$C_R = 2G/(\rho V^2 S) \tag{3.33}$$

In the context of the equation mentioned, V typically stands for the true speed of the Solar Powered Unmanned Aerial Vehicle (SPUAV), and S represents the reference area. The vertical velocity during climbing and descending can be expressed as follows:

$$V_V = \sqrt{(2G/\rho S)}.(C_T - C_D)/C_R^{3/2} \tag{3.34}$$

The power required in flight is defined as

$$P_{flight} = \sqrt{2G^3/\rho S}\,.\,C_T/C_R^{3/2} \tag{3.35}$$

3.1.12 The Daily Electrical Energy Equilibrium

Sustaining the aircraft's operations relies on ensuring that the energy collected from the solar cells throughout the day is at least equal to the electrical energy needed by the aircraft. This balance is of utmost importance.

3.1.13 The Daily Solar Energy Collected

The solar energy received at a particular moment is outlined as follows.

$$P_{Solar} = SI_h \sin\alpha \;\; S_{Solar}\eta_{Solar}\eta_{Manager} \tag{3.36}$$

Significant parameters in this context include the efficiency achieved for the solar cells, denoted as η_{Solar}, and the efficiency of the DC/DC converter controlled by the energy management system, $\eta_{Manager}$. It's worth emphasizing that the design of the cambered airfoil, wing installation angle, and aircraft attitude angle can have an impact on the absorption of solar irradiance. In this design approach, the solar panels are set to a flat orientation, which results in a different definition of the surface covered by the solar panels. S_{Solar} is now redefined as the projection of the solar panels onto a specific plane. Consequently, k_{Solar} needs to be adjusted, making it slightly larger than its actual value. The total solar energy harvested in a day can then be calculated as follows.

$$E_{Solar} = \oint_{day} P_{Solar}\ dt \tag{3.37}$$

For estimating the charging energy concerning the battery, two key factors are needed: the charge efficiency, denoted as η_{charge}, and the total power consumption of the SPUAV platform systems, represented as P_{Need}. The charging energy can be calculated as follows.

$$E_{Solar} = \oint_{P_{Solar} > \mathrm{P_{Need}}} \eta_{charge}(P_{Solar} - \mathrm{P_{Need}})\ dt \tag{3.38}$$

The overall power consumption of the Small Unmanned Aerial Vehicle (SPUAV) platform encompasses the propulsion system, avionics, and payload. The power requirements for avionics, referred to as $P_{Avionics}$, and payload, denoted as $P_{Payload}$, remain constant. It's crucial to consider variations in the line loss rate and voltage for these two components. The efficiency factor, η_{bec}, should be factored into account for these fluctuations. The power input necessary for the propulsion system is represented as P_{Prop}. Consequently, the total electrical power consumption of the SPUAV platform can be expressed as follows:

$$P_{Needs} = P_{Prop} + (P_{Avionics} + P_{Payload})/\eta_{bec} \tag{3.39}$$

3.1.14 The Daily Electrical Energy Demand

The daily electrical energy requirement can be divided into two scenarios: when the solar power exceeds the total power requirement, and when the solar power falls short of the total power requirement. During the transitional periods of dusk and dawn, when solar power is insufficient, both sources - the solar cells and the battery - are utilized. The shift between these sources is gradual. The calculation of daily energy consumption takes into account the total power consumption, incorporating the battery's charging efficiency, η_{charge}, and discharging efficiency, $\eta_{dcharge}$, for the nighttime period. If we are calculating the energy solely derived from the battery, without the contribution from solar panels, the calculation is as follows.

$$E_{dcharge} = \oint_{P_{Solar} \le \mathrm{P_{Need}}} (\mathrm{P_{Need}} - P_{Solar})/(\eta_{dcharge}\ \eta_{Manager})\ dt \tag{3.40}$$

When solar power is above the total required power, the energy required is:

$$E_{day} = \oint_{P_{Solar} > \mathrm{P_{Need}}} \mathrm{P_{Need}}\ dt \tag{3.41}$$

During transitional periods when available solar irradiation dips below the cumulative demands of onboard systems, a graduated switching protocol engages, progressively supplementing photovoltaic generation with stored chemical energy from batteries to compensate for deficits. The algorithm factors in cell charge-discharge efficiencies, regulating power flow to sustain continuous, uninterrupted UAV functionality throughout diurnal cycles. Subsequently, the total daily electrical load is computed by integrating the photovoltaic and battery contributions to instantiate an equilibrium.

$$E_{Need} = E_{Day} + E_{dcharge}/\eta_{dcharge} + \oint_{P_{Solar} \leq P_{Need}} P_{Solar}\ dt \qquad (3.42)$$

3.1.15 Mission Achievements

The specifications for the High-Altitude Long Endurance Solar-Powered (SPUAV) have been able to compass the following:

a. Capable of sustained flight for a minimum duration of 720 hours (equivalent to 30 days) post-launch. Reach a maximum altitude of 65,000 feet (during 30-day flight).

b. Achieve a peak flying height of up to 65,000 feet during its 30-day airborne period.

c. Maintain a flight level not lower than 40,000 feet throughout the 30-day journey.

d. Operate independently using renewable energy sources for the entire duration of the 30-day flight.

3.1.16 Mission Profile

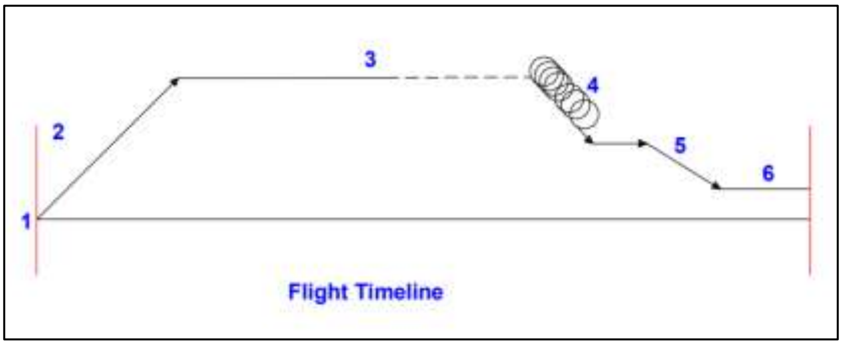

Figure 3.9: Mission Profile.

The Flight should follow the following steps as shown in the figure above:

i. Take-off

ii. Reaching maximum altitude

iii. Flying through the daytime oar night at certain level
iv. Loitering descent
v. Final descent in flight level
vi. Landing

3.2 SOLAR POWER CALCULATIONS

3.2.1 The Radiation From The Sun

Solar radiation refers to the emission of energy from the sun onto a designated surface, such as Earth. The harnessing of solar energy has ancient origins, being utilized for activities like igniting fires, boiling water, and cooking food. A pivotal moment occurred in 1839 when French Physicist Alexander-Edmond Becquerel discovered the Photovoltaic Effect, enabling the conversion of solar energy into electricity. In 1883, Charles Fritts achieved a significant milestone by coating a Selenium semiconductor with a thin layer of gold, creating the first solar cell with a modest efficiency of 1%. Fast forward to 1954, the development of the first silicon photovoltaic (PV) solar cell showcased an efficiency of approximately 4%. Today, solar cell efficiencies range from 18% to 40%, demonstrating substantial advancements. The improvement in solar cell performance has been accompanied by a notable decrease in costs. This decline in costs is a direct consequence of increased solar cell production. The average solar radiation received at the edge of Earth's atmosphere, commonly known as Total Solar Irradiance, is approximately $1361\ W/m^2$.

Table 3.3: Solar Radiation Values.

Solar Radiation per month of the year in turkey $KWh/m^2 - month$			
January	51.75	**July**	175.38
February	63.27	**August**	158.40
March	96.65	**September**	123.28
April	122.23	**October**	89.90
May	153.86	**November**	60.82
June	168.75	**December**	46.87
Total	1311		

Note: values depend on position at earth/ the above values were taken from Republic of Türkiye Ministry of Energy and Natural Resources.

The quantity of solar radiation reaching a particular area is typically diminished by about 50% as it traverses our atmosphere. Despite this reduction, the actual solar energy that reaches the Earth's surface surpasses total energy consumption. Losses in the solar spectrum primarily occur due to absorption and reflection, along with scattering caused by water vapor and carbon dioxide present in our atmosphere.

3.2.2 Solar Cell Selection

Solar cells come in various types, typically crafted from semiconductor materials, with Silicon being the most common albeit relatively expensive. Advances in solar technology have introduced a diverse range of lightweight and highly efficient solar cells. Among these, multi-junction solar cells are prevalent, featuring a stacked design with a single junction over another. Such high-efficiency solar cells find primary applications in spacecraft. For this project, the SunPower C60 solar cell is selected, boasting an efficiency of around 22.5% and a notable reduction in weight compared to other cells with similar efficiencies. The table below outlines some of the most used solar cells in various markets, including their specifications and efficiency ratings.

Table 3.4: Solar Cells Kinds and Specifications.

Solar Cell Markets Anaysis									
	Length	Breadth	Thick-ness	Voc	Isc	Vmp	Imp	Power	Effic-iency
Sun Power A300	125.0	125.0	0.3	0.7	5.9	0.6	5.5	3.1	21.5
RC7 2-75 Flex Solar Cell	270	90.0	0.2	10.5	0.1	7.2	0.1	0.7	3.0
Wave Sol Ascent solar 1.1	1148	330	NA	23.0	1.9	15.8	1.4	21.0	5.5
NanoSolar NanoCell 26 watt	165.0	135.0	0.4	0.6	6.7	0.5	5.8	2.6	11.7
DIY 0.5W2V/ 330MA	194.0	60.0	NA	1.5	0.3	NA	NA	0.5	4.3
Sun power C60	125.0	125.0	0.2	0.7	6.3	0.6	5.9	3.4	22.5
IXOLARTM High Efficiency SolarBIT	22.0	7.0	1.8	0.6	0.1	0.5	0.0	0.0	22.0
Spectro Lab	80.0	40.0	0.1	2.7	0.5	2.4	0.5	1.2	28.3

3.2.3 Rechargeable Batteries

The energy collected from the solar cells during daytime hours may be stored within the on-board batteries to be used for night flight. Since the batteries used are critical, an analysis of various battery types was conducted, and is shown in Table below. The types of batteries taken under consideration are Lead-Acid, Lithium-Ion, Nickel-Cadmium, and Lithium-Polymer; all of which are capable of being fully recharged.

Table 3.5: Batteries Kinds.

Advantages and Disadvantages of various Battery Types		
Type	Advantage	Disadvantage
Lead Acid	1.Their technology is well-established, with a long history of reliable use and understanding. 2. boast high recyclability. 3. durability and resilience. 4. ensure easy sourcing for a variety of applications.	1. exhibit lower energy density. 2. tend to be heavier and bulkier. 3. The number of charge-discharge cycles is relatively limited. 4. require regular maintenance.
Lithium-Ion	1. exhibit a high energy density, providing a greater storage capacity per unit weight and volume. 2. longer cycle. 3. can be charged at a faster. 4. Lightweight and compact.	1. more expensive. 2. Performance can be affected by temperature extremes. 3. can pose safety risks. 4. their performance may degrade over time, especially if not used regularly.
Nickel-Cadmium	1. high charge and discharge efficiency. 2. long life cycle. 3. robust and durable. 4. Operate effectively across a broad temperature range.	1. toxic nature of cadmium. 2. may experience memory effect. 3. lower energy density. 4. can lose charge when not in use.
Lithium-Polymer	1. offer a high energy density, providing a greater storage capacity per unit weight. 2. flexible form factor. 3. lightweight. 4. exhibit a low self-discharge rate.	1. sensitive to temperature fluctuations. 2. Overcharging or improper usage may lead to swelling or bloating of lithium polymer. 3. higher production costs. 4. lifespan of lithium polymer batteries is limited.

Due to the relatively slow advancement in rechargeable battery technology in recent years, the energy density remains comparatively low, and these batteries can be excessively heavy. In this study we will use lithium-Ion because we have larger UAV with a need for higher energy density and longer flight times, Li-ion batteries might be more suitable.

3.2.4 Prototype Conditions

i. UAV Weight: Maximum take-off weight of the aircraft should be 20kg.

ii. Load Weight: The UAV has to carry the payload of 5kg to 10 kg.

iii. Endurance: Endurance of this UAV should be greater than 10 hours. To further increase the endurance, solar cells will be installed on UAV surfaces to produce the power needed.

iv. Altitude of Flying: The UAV is designed for high altitudes so it will be flying between 1 to 5 km above the ground.

4. RESULTS AND DISCUSSION

In this chapter, the results of the study, whose steps were explained in the previous chapter, will be reviewed. Where the results will be reviewed in this chapter, and the results are the results of enhanced endurance of UAV with selected model MQ-9 after placing solar panels on the wing, the solar panels were placed on the whole body of the wing. Then the energy harvested from the sun will be calculated and added to total energy of the Solar Powered Unmanned Aerial Vehicle.

4.1 THE SELSCTED SOLAR PANELS SPECIFICATIONS

Solar cells produce zero carbon emissions, rendering them a highly promising and environmentally friendly power source.so our model has large wingspan equal to $20\ meters$ that makes the benefit of solar power very high. we have selected the best solar cells that has the maximum efficiency and lighter weight and provide secondary power source to the SPUAV. Here are the properties of sunpower C60 Si Monocrystalline where the efficiency is equal to $22.9 \pm 0.6\ \cong 23\ \%$ but after placing at the SPUAV the raquiered efficiency was equal to $20\ \%$. And sunpower C60 Si Monocrystalline is less costing than other types. The solar cell is often modelled as a current source (I_L) in parallel with a diode. To account for real-world imperfections, a shunt resistance (R_{SHS}) and a series resistance (R_{SRS}) are introduced into the model (Lorenzo E, 1994). The equivalent circuit of a solar cell is illustrated in Figure 4.1. When a solar cell is short-circuited, the current reaches its maximum value (I_{SC}), while the voltage drops to zero, resulting in zero power. As the load impedance increases, the current remains relatively constant and then starts to decrease (from I_M), while the voltage continues to rise until reaching V_M. At open circuit, the voltage is at its maximum (V_{OC}), but the current is zero[48]. The power delivered by the solar cell to the load is the product of voltage and current, and this behavior is depicted in Fig 4.2 with respect to irradiance, load, and temperature. To utilize the solar cell most efficiently, it is crucial to operate around this maximum power point, and the circuitry used for tracking the maximum power point is essential. The typical efficiency of Maximum Power Point Tracking (MPPT) is approximately 94% to 98% . The solar cells installed in MQ9 are SunPower C60, and the characteristics of SunPower C60 are provided in Table 4.1 [48].

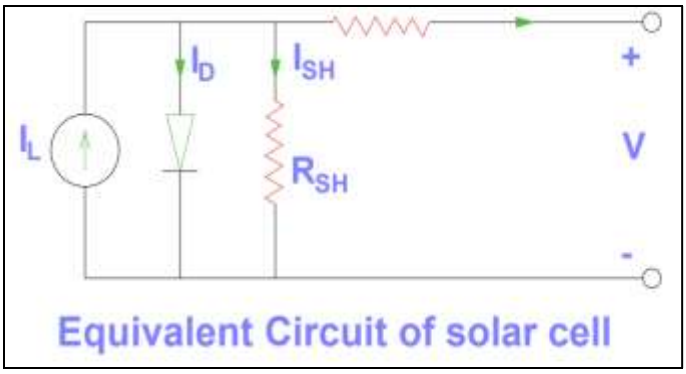

Figure 4.1: **E**quivalent Circuit of a Solar Cell.

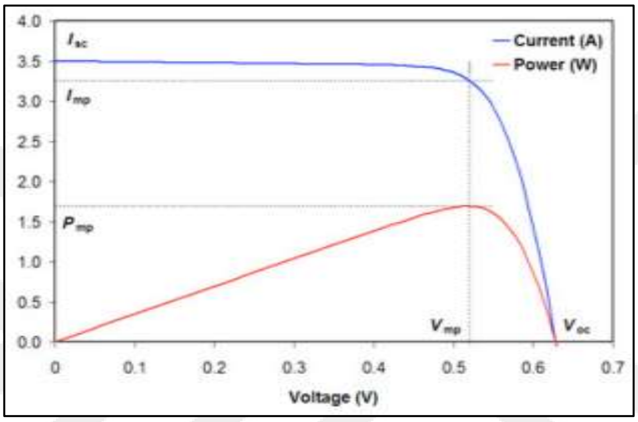

Figure 4.2: Performance Curves Of A Solar Cell Showing The Variation Of Current And Power With Voltage Under Specific Irradiance, Load, And Temperature Conditions.

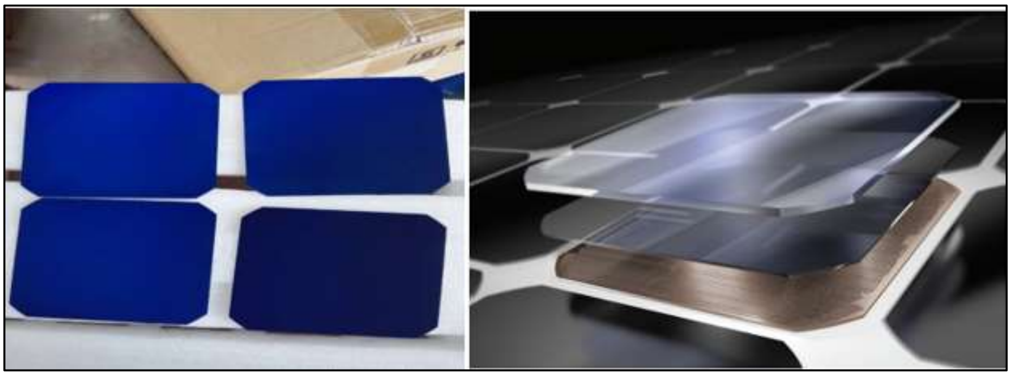

Figure 4.3: Sunpower C60.

Table 4.1: SunPower C60 Specifications.

Parameter	Value
Peak Power	3.42 $watt$
Efficiency	22.5 %
Peak Voltage	0.582 $volt$
Peak Current	5.93 $amper$
Open-Circuit Voltage	0.687 $volt$
Short-Circuit Voltage	6.28 $volt$
Length	12.5 mm
Width	12.5 mm
Thickness	0.165 mm
Mass	0.008 kg

4.2 SOLAR PANELS APPLICATION ON UAV WING

The MQ9 wing was fully covered with Photovoltaic cells SunPower c60 like the following.

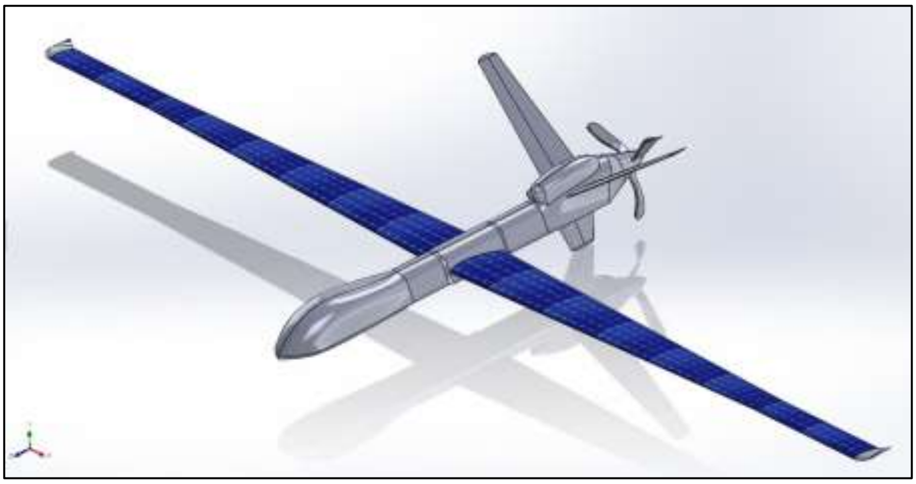

Figure 4.4: SunPower C60 Cells Placed on MQ9 Wing.

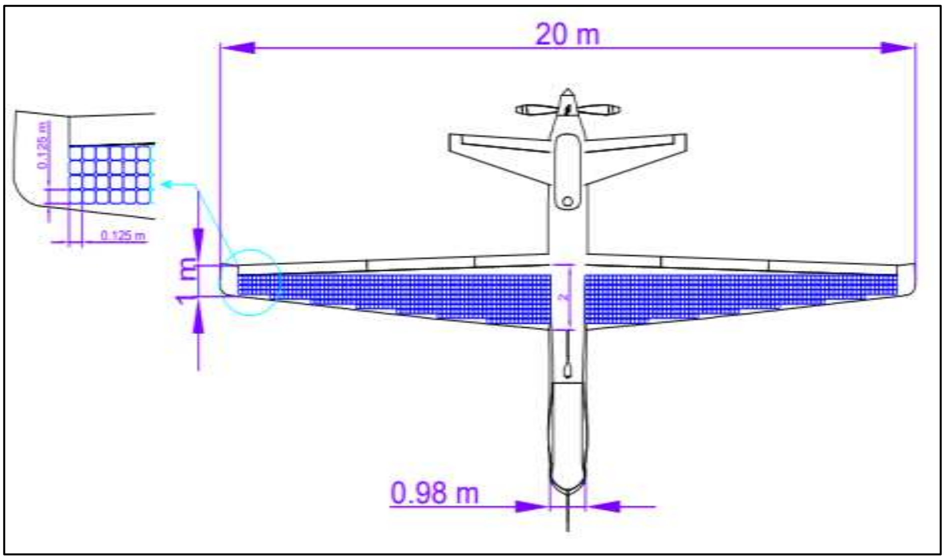

Figure 4.5: MQ9 Solar Cells Diagram.

The MQ9 has wing span area equal to 16.38 $m^2$where the single photovoltaic cell area is equal to: $A_{PV} = 0.125 \times 0.125 = 0.015625\ m^2$

that means we are able to place the following number of cells.

$$N = \frac{A_{WING}}{A_{PV}} = \frac{16.38\ m^2}{0.015625\ m^2} = 1048\ cells$$

Placed on the wing of the SPUAV MQ9, The total PV cells weight is equal to

$$M_{tot} = M_{PV} \times N = 0.008 \times 1048 = 8.4\ kg$$

The Connection of the Photovoltaic Cells is in series and forms a Single PV array.

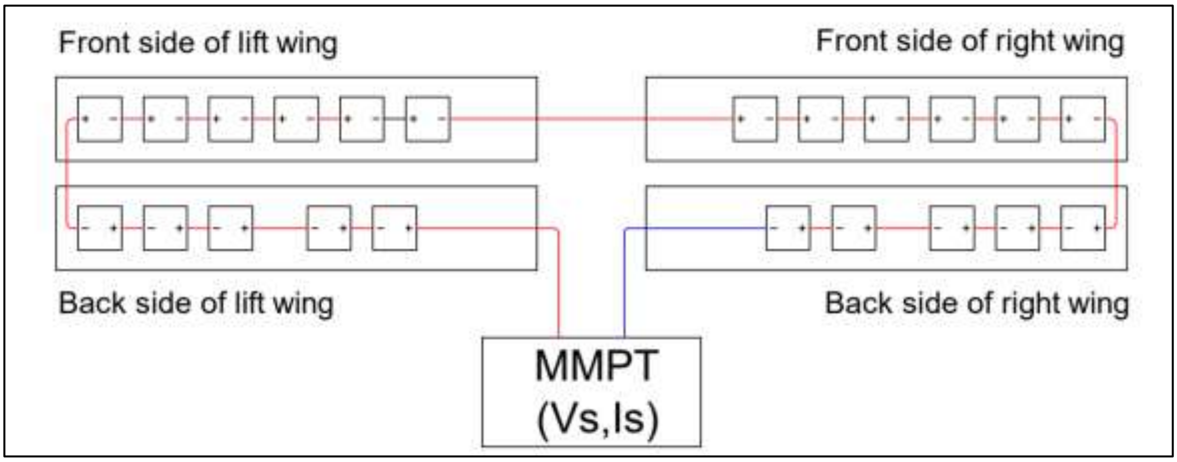

Figure 4.6: Array Connection in Power System.

The Total voltage and Current produced from the Photovoltaic cells are like the following taking in consideration the voltage produced by one cell as manufacturer $0.5\ V$ where the solar radiation is between $300\ to\ 1000\frac{W}{m^2}$ in the highest day of the year in solar radiation at the middle of the day $12.00\ pm$:

$$V_{mp} = V_{tot} = V_{PV} \times N = 0.5\ \times 1048 = \ 524\ V$$

$$I_{mp} = I_{tot} = I_{PV} \times N = 5.9\ \times 1048 = \ 6180\ A$$

Hence the Total electrical power produced by the solar system at midday in a perfectly sunny day taking in consideration the efficiency of the system:

$$P_{solar} = I_{tot} \times V_{tot}$$

Now, it is known that the solar irradiance on earth is equal to $340\frac{W}{m^2}$at the top of the atmosphere without defining certain country, because MQ9 SPUAV will cruise over many countries, now to convert from $\frac{W}{m^2}$to $\frac{KWh}{m^2-day}$ we multiply by 0.024, so the total irradiance per day is $340 \times 0.024 = 8.16\ \frac{KWh}{m^2-day}$

Total Power from the Solar panels is the solar irradiance multiplied by the solar panels area

$$P_{PV} = 8.16\ \times A_{WING} = 8.16\ \times 16.38 = \ 133.7\ \frac{KWh}{day}$$

Now to calculate the $Capacity_{battery}$of the battery required to store the energy per day taking in consideration the losts is LI-Ion batteries equal to 5% and taking 1.5 factor to compensate low winter temperatures and the inefficiency of the Inverter equal to 10% so

$$Size_{battery} = P_{PV}\left(\frac{KWh}{day}\right) \times consumptionfactor \times \eta_{LI-ION} \times \eta_{inverter} \times \eta_{discharge}$$

$$Size_{battery} = 133.7 \times 1.5 \times 1.05 \times 1.1 \times 1.2 = \ 278\ \frac{KWh}{day}$$

$$Capacity_{battery} = \frac{Size_{battery}\ \frac{KWh}{day}\ \times 1000}{volt} = \frac{278000}{24} = 11580\ Ah$$

Taking in consideration the efficiency of the system

$$P_{PVactual} = P_{PV} \times E = 133.7 \times 0.225 = 30\ KWh$$

The mission of MQ9 is determined to be $24\ hours$ long, taking in consideration the sun irradiation is equal to 7 hours in its average value, so the total gained power from the solar cells is

$$P_{PVfinal} = P_{PVactual} \times time = 30 * 7 = 210\ KW$$

It is known that the MQ9 has $712\ kW$ engine So the new capacity after adding the solar capacity will be

$$P_{real} = P_{electrical} + P_{PVfinal} = 712 + 210 = 922\ KW$$

When the capacity of MQ9 was $712\ KW$ the range was $1850\ km$, so with new capacity equal to $922\ KW$ the new range is

$$R_{new} = \frac{1850\ km \times 922\ KW}{712\ KW} = 2395\ km$$

That means a total enhanced endurance ration equal to

$$Enhanced\ Ratio = \frac{2395\ km - 1850\ km}{1850\ km} = 0.2945\ \% \Rightarrow Enhanced\ Ratio\ is\ 29\ \%$$

So, the operation of covering the wing of MQ9 UAV with Sunpower c60 PV and converting the UAV to be SPUAV made an improvement in the performance of the SPUAV close to 30 %.

So, in large wingspan UAVs it is beneficial to cover the wing with solar cells that will reduce costs and enhance the performance of the UAV.

In the future all the UAVs should be supplied with clean and sustainable power source which is the sun especially with the current problems in finding fuel.

5. CONCLUSIONS AND FUTURE WORK

5.1 CONCLUSIONS

In conclusion, the innovative implementation of SunPower C60 photovoltaic cells on the MQ-9's wing has markedly improved the UAV's operational efficiency. By fully covering the MQ9 wing with these high-efficiency solar cells, we have successfully harnessed solar energy to augment the UAV's power source. The results of our study reveal a substantial increase in the endurance of the Solar Powered Unmanned Aerial Vehicle (SPUAV), with a performance enhancement close to 30%. This significant improvement is attributed to the additional electrical power generated by the solar panels under optimal conditions, contributing effectively to the UAV's total energy capacity. These findings underscore the potential benefits of incorporating renewable energy sources in UAV technology. Our research not only demonstrates the feasibility of solar energy integration in enhancing UAV endurance but also paves the way for future advancements in UAV technology, advocating for a shift towards more sustainable and efficient power solutions. This approach, capitalizing on solar energy, is particularly crucial in the context of contemporary challenges associated with fuel availability and environmental sustainability. The successful application of solar panels on the MQ-9 UAV serves as a promising model for future endeavors in the field, highlighting the potential of solar energy in revolutionizing UAV operations.

5.2 FUTURE WORK

i. Advanced Solar Technology Integration:

   Focus on integrating cutting-edge solar technologies into various UAV models, utilizing more efficient, flexible, and lighter solar panels.

ii. Enhanced Energy Storage and Management:

   Develop advanced energy storage systems, like high-density batteries or supercapacitors, to store excess energy from solar panels.

iii. Extending Operational Endurance of UAVs:

Work on increasing the flight duration of solar-powered UAVs by optimizing design for energy efficiency and testing in long-range surveillance missions.

iv. Exploration of Solar Applications in Aerospace:

Explore the potential of solar technology in broader aerospace applications, assessing its viability in larger aircraft and its impact on environmental sustainability.

REFERENCES

[1] Consortiq, “A Not-So-Short History of Unmanned Aerial Vehicles (UAV),” consortiq. [Online]. Available: https://consortiq.com/

[2] M. Palik and M. Nagy, “Brief history of UAV development,” *Repüléstudományi Közlemények*, vol. 31, no. 1, pp. 155–166, 2019, doi: 10.32560/rk.2019.1.13.

[3] A. & S. Magazine, “History, Travel, Arts, Science, People, Places Smithsonian Magazine,” Air & Space Magazine. [Online]. Available: https://www.smithsonianmag.com/

[4] P. S. University, “UAS History | GEOG 892: Unmanned Aerial Systems,” Penn State University. [Online]. Available: https://dutton.psu.edu/

[5] Frontiers, “A Survey on Operation Concept, Advancements, and Applications of UAVs,” Frontiers. [Online]. Available: https://www.frontiersin.org/

[6] A. A. Laghari, A. K. Jumani, R. A. Laghari, and H. Nawaz, “Unmanned aerial vehicles: A review,” *Cognitive Robotics*, vol. 3. KeAi Communications Co., pp. 8–22, Jan. 01, 2023. doi: 10.1016/j.cogr.2022.12.004.

[7] X. LI, K. SUN, and F. LI, “General optimal design of solar-powered unmanned aerial vehicle for priority considering propulsion system,” *Chinese Journal of Aeronautics*, vol. 33, no. 8. Chinese Journal of Aeronautics, pp. 2176–2188, Aug. 01, 2020. doi: 10.1016/j.cja.2020.04.009.

[8] C. Zhang *et al.*, “A comprehensive review of electrochemical hybrid power supply systems and intelligent energy managements for unmanned aerial vehicles in public services,” *Energy and AI*, vol. 9, Aug. 2022, doi: 10.1016/j.egyai.2022.100175.

[9] R. D’Sa *et al.*, “SUAV: Q - An improved design for a transformable solar-powered UAV,” *IEEE International Conference on Intelligent Robots and Systems*, vol. 2016-Novem, pp. 1609–1615, 2016, doi: 10.1109/IROS.2016.7759260.

[10] R. D. Sa, D. Jenson, and N. Papanikolopoulos, “SUAV: Q - A Hybrid Approach To Solar-Powered Flight,” pp. 3288–3294, 2016.

[11] V. Cipolla, A. Dine, A. Viti, and V. Binante, "MDAO and Aeroelastic Analyses of Small Solar-Powered UAVs with Box-Wing and Tandem-Wing Architectures," *Aerospace*, vol. 10, no. 2, pp. 1–22, 2023, doi: 10.3390/aerospace10020105.

[12] Z. Guo, X. K. Chen, Z. X. Hou, and J. Guo, "Development of a solar electric powered UAV for long endurance flight," *11th AIAA Aviation Technology, Integration, and Operations (ATIO) Conference, including the AIAA Balloon Systems Conference and 19th AIAA Lighter-Than-Air Technology Conference*, no. September, pp. 1–13, 2011, doi: 10.2514/6.2011-6966.

[13] X. Zhu, Z. Guo, and Z. Hou, "Solar-powered airplanes: A historical perspective and future challenges," *Progress in Aerospace Sciences*, vol. 71, pp. 36–53, 2014, doi: 10.1016/j.paerosci.2014.06.003.

[14] R. Dai, U. Lee, S. Hosseini, and M. Mesbahi, "Optimal path planning for solar-powered UAVs based on unit quaternions," *Proceedings of the IEEE Conference on Decision and Control*, pp. 3104–3109, 2012, doi: 10.1109/CDC.2012.6425972.

[15] I. Ridwan and Alfindo, "The effect of use of solar panels on micro scale fixed-wing UAV type as a power recharging system," *AIP Conf Proc*, vol. 2180, no. December 2019, doi: 10.1063/1.5135553.

[16] P. Oettershagen *et al.*, "A solar-powered hand-launchable UAV for low-altitude multi-day continuous flight," *Proc IEEE Int Conf Robot Autom*, vol. 2015-June, no. June, pp. 3986–3993, 2015, doi: 10.1109/ICRA.2015.7139756.

[17] Z. Tian, Z. J. Haas, and S. Shinde, "Routing in Solar-Powered UAV Delivery System," *Drones*, vol. 6, no. 10, 2022, doi: 10.3390/drones6100282.

[18] A. J. R. Malaver, L. F. Gonzalez, N. Motta, and T. F. Villa, "Design and flight testing of an integrated solar powered UAV and WSN for remote gas sensing," *IEEE Aerospace Conference Proceedings*, vol. 2015-June, pp. 1–10, 2015, doi: 10.1109/AERO.2015.7119209.

[19] T. Muskardin, G. Balmer, S. Wlach, K. Kondak, M. Laiacker, and A. Ollero, "Landing of a fixed-wing UAV on a mobile ground vehicle," *Proc IEEE Int Conf*

Robot Autom, vol. 2016-June, pp. 1237–1242, 2016, doi: 10.1109/ICRA.2016.7487254.

[20] S. Morton, R. D'Sa, and N. Papanikolopoulos, "Solar powered UAV: Design and experiments," *IEEE International Conference on Intelligent Robots and Systems*, vol. 2015-Decem, pp. 2460–2466, 2015, doi: 10.1109/IROS.2015.7353711.

[21] R. D'Sa *et al.*, "Design and experiments for a transformable solar-UAV," *Proc IEEE Int Conf Robot Autom*, pp. 3917–3923, 2017, doi: 10.1109/ICRA.2017.7989451.

[22] R. Chen, X. Zhu, Z. Zhou, Z. Wang, and T. Zhang, "Study on the structure design of solar powered UAV," *2018 IEEE International Conference on Prognostics and Health Management, ICPHM 2018*, no. 1, 2018, doi: 10.1109/ICPHM.2018.8448618.

[23] Y. Chen, "Overview of Solar UAV Power System," *Academic Journal of Science and Technology*, vol. 4, no. 1, pp. 80–82, 2022, doi: 10.54097/ajst. v4i1.3258.

[24] A. A. Alsahlani, L. J. Johnston, and P. A. Atcliffe, "Design of a high-altitude long endurance flying-wing solar-powered unmanned air vehicle," no. July 2015, pp. 3–24, 2017, doi: 10.1051/eucass/201609003.

[25] M. Peciak, W. Skarka, K. Mateja, and M. Gude, "Impact Analysis of Solar Cells on Vertical Take-Off and Landing (VTOL) Fixed-Wing UAV," *Aerospace*, vol. 10, no. 3, 2023, doi: 10.3390/aerospace10030247.

[26] L. Sai, Z. Wei, and W. X. 601, "The Development Status and Key Technologies of Solar Powered Unmanned Air Vehicle," in *IOP Conf Series: Material Science and Engineering*, 2016. doi: 10.1088/1742-6596/755/1/011001.

[27] P. Agnihotri, S. Pavan, T. Kunche, and A. K. Mishra, "Design and Development of Solar Powered UAV for Long Endurance Design and Development of Solar Powered UAV for Long Endurance," no. March 2022.

[28] X. Zhao, Z. Zhou, X. Zhu, and A. Guo, "Design of a hand-launched solar-powered unmanned aerial vehicle (UAV) system for plateau," *Applied Sciences (Switzerland)*, vol. 10, no. 4, 2020, doi: 10.3390/app10041300.

[29] A. Alsahlani, T. Rahulan, and N. Abdulhassan, “Composite structural analysis of a high altitude, solar powered unmanned aerial vehicle,” *International Journal of Mechanical Engineering and Robotics Research*, vol. 6, no. 1, pp. 71–76, 2017, doi: 10.18178/ijmerr.6.1.71-76.

[30] C. Thipyopas, V. Sripawadkul, and N. Warin, “Design and Development of a Small Solar-Powered UAV for Environmental Monitoring Application,” *2019 IEEE Eurasia Conference on IOT, Communication and Engineering, ECICE 2019*, pp. 316–319, 2019, doi: 10.1109/ECICE47484.2019.8942777.

[31] A. Haider, “PERPETUAL FLIGHT FOR SURVEILLANCE OF LONG- DISTANCE GAS DESIGN OF SOLAR POWERED UNMANNED AERIAL VEHICLE WITH PERPETUAL FLIGHT FOR SURVEILLANCE OF LONG-,” no. August, pp. 0–1, 2022.

[32] P. Oettershagen *et al.*, “Design of small hand-launched solar-powered UAVs: From concept study to a multi-day world endurance record flight,” *J Field Robot*, vol. 34, no. 7, pp. 1352–1377, 2017, doi: 10.1002/rob.21717.

[33] T. LEI, Z. YANG, Z. LIN, and X. ZHANG, “State of art on energy management strategy for hybrid-powered unmanned aerial vehicle,” *Chinese Journal of Aeronautics*, vol. 32, no. 6, pp. 1488–1503, 2019, doi: 10.1016/j.cja.2019.03.013.

[34] N. V. Nguyen, J. W. Lee, M. Tyan, and D. Lee, “Possibility-based multidisciplinary optimisation for electric-powered unmanned aerial vehicle design,” *Aeronautical Journal*, vol. 119, no. 1221, pp. 1397–1414, 2015, doi: 10.1017/S0001924000011313.

[35] G. De Carvalho Bertoli, G. M. Pacheco, and G. J. Adabo, “Extending flight endurance of electric unmanned aerial vehicles through photovoltaic system integration,” *2015 International Conference on Renewable Energy Research and Applications, ICRERA 2015*, vol. 5, pp. 143–147, 2015, doi: 10.1109/ICRERA.2015.7418556.

[36] A. Guo, Z. Zhou, X. Zhu, X. Zhao, and Y. Ding, “Automatic control and model verification for a small aileron-less hand-launched solar-powered unmanned aerial

vehicle," *Electronics (Switzerland)*, vol. 9, no. 2, 2020, doi: 10.3390/electronics9020364.

[37] X. LI, K. SUN, and F. LI, "General optimal design of solar-powered unmanned aerial vehicle for priority considering propulsion system," *Chinese Journal of Aeronautics*, vol. 33, no. 8, pp. 2176–2188, 2020, doi: 10.1016/j.cja.2020.04.009.

[38] Y. Hu, Y. Yang, X. Ma, and S. Li, "Computational optimal launching control for balloon-borne solar-powered unmanned aerial vehicles in near-space," *Sci Prog*, vol. 103, no. 1, 2020, doi: 10.1177/0036850419877755.

[39] A. Hamza, A. Mohammed, and A. Isah, "Towards Solar-Powered Unmanned Aerial Vehicles for Improved Flight Performance," *2019 2nd International Conference of the IEEE Nigeria Computer Chapter, NigeriaComputConf 2019*, pp. 1–5, 2019, doi: 10.1109/NigeriaComputConf45974.2019.8949672.

[40] P. Oettershagen *et al.*, "Long-endurance sensing and mapping using a hand-launchable solar-powered UAV," *Springer Tracts in Advanced Robotics*, vol. 113, pp. 441–454, 2016, doi: 10.1007/978-3-319-27702-8_29.

[41] Y. Sun, D. Wing Kwan Ng, D. Xu, L. Dai, and R. Schober, "Resource Allocation for Solar Powered UAV Communication Systems," *IEEE Workshop on Signal Processing Advances in Wireless Communications, SPAWC*, vol. 2018-June, pp. 1–5, 2018, doi: 10.1109/SPAWC.2018.8445944.

[42] Y. Huang, J. Chen, H. Wang, and G. Su, "A method of 3D path planning for solar-powered UAV with fixed target and solar tracking," *Aerosp Sci Technol*, vol. 92, pp. 831–838, 2019, doi: 10.1016/j.ast.2019.06.027.

[43] Y. Sun, D. Xu, D. W. K. Ng, L. Dai, and R. Schober, "Optimal 3D-Trajectory Design and Resource Allocation for Solar-Powered UAV Communication Systems," *IEEE Transactions on Communications*, vol. 67, no. 6, pp. 4281–4298, 2019, doi: 10.1109/TCOMM.2019.2900630.

[44] V. S. Dwivedi, J. Patrikar, A. Addamane, and A. K. Ghosh, "MARAAL: A Low Altitude Long Endurance Solar Powered UAV for Surveillance and Mapping

Applications," *2018 23rd International Conference on Methods and Models in Automation and Robotics, MMAR 2018*, pp. 449–454, 2018, doi: 10.1109/MMAR.2018.8485805.

[45] M. Wu, Z. Shi, T. Xiao, and H. Ang, "Energy optimization and investigation for Z-shaped sun-tracking morphing-wing solar-powered UAV," *Aerosp Sci Technol*, vol. 91, pp. 1–11, 2019, doi: 10.1016/j.ast.2019.05.013.

[46] M. El Adawy *et al.*, "Design and fabrication of a fixed-wing Unmanned Aerial Vehicle (UAV)," *Ain Shams Engineering Journal*, vol. 14, no. 9, Sep. 2023, doi: 10.1016/j.asej.2022.102094.

[47] X. LI, K. SUN, and F. LI, "General optimal design of solar-powered unmanned aerial vehicle for priority considering propulsion system," *Chinese Journal of Aeronautics*, vol. 33, no. 8. Chinese Journal of Aeronautics, pp. 2176–2188, Aug. 01, 2020. doi: 10.1016/j.cja.2020.04.009.

[48] V. S. Dwivedi, P. Kumar, A. K. Ghosh, and G. M. Kamath, "Selection of Size of Battery for Solar Powered Aircraft," Elsevier B.V., Jan. 2018, pp. 424–430. doi: 10.1016/j.ifacol.2018.09.450.